EUROPEAN ORGANIZATION FOR NUCLEAR RESEARCH (CERN)

CERN-PH-EP/2012-029
2012/09/14

CMS-SUS-11-021

Search for physics beyond the standard model in events with a Z boson, jets, and missing transverse energy in pp collisions at $\sqrt{s} = 7$ TeV

The CMS Collaboration*

Abstract

A search is presented for physics beyond the standard model (BSM) in events with a Z boson, jets, and missing transverse energy ($E_{\mathrm{T}}^{\mathrm{miss}}$). This signature is motivated by BSM physics scenarios, including supersymmetry. The study is performed using a sample of proton-proton collision data collected at $\sqrt{s} = 7$ TeV with the CMS experiment at the LHC, corresponding to an integrated luminosity of 4.98 fb^{-1}. The contributions from the dominant standard model backgrounds are estimated from data using two complementary strategies, the jet-Z balance technique and a method based on modeling $E_{\mathrm{T}}^{\mathrm{miss}}$ with data control samples. In the absence of evidence for BSM physics, we set limits on the non-standard-model contributions to event yields in the signal regions and interpret the results in the context of simplified model spectra. Additional information is provided to facilitate tests of other BSM physics models.

Submitted to Physics Letters B

*See Appendix B for the list of collaboration members

1 Introduction

This paper describes a search for physics beyond the standard model (BSM) in proton-proton collisions at a center-of-mass energy of 7 TeV. Results are reported from a data sample collected with the Compact Muon Solenoid (CMS) detector at the Large Hadron Collider (LHC) at CERN corresponding to an integrated luminosity of $4.98\,\mathrm{fb}^{-1}$. This search is part of a broad program of inclusive, signature-based searches for BSM physics at CMS, characterized by the number and type of objects in the final state. Since it is not known a priori how the BSM physics will be manifest, we perform searches in events containing jets and missing transverse energy ($E_{\mathrm{T}}^{\mathrm{miss}}$) [1–3], single isolated leptons [4], pairs of opposite-sign [5] and same-sign [6] isolated leptons, photons [7, 8], etc. Here we search for evidence of BSM physics in final states containing a Z boson that decays to a pair of oppositely-charged isolated electrons or muons. Searches for BSM physics in events containing oppositely-charged leptons have also been performed by the ATLAS collaboration [9–11].

This strategy offers two advantages with respect to other searches. First, the requirement of a leptonically-decaying Z boson significantly suppresses large standard model (SM) backgrounds including QCD multijet production, events containing Z bosons decaying to a pair of invisible neutrinos, and events containing leptonically-decaying W bosons, and hence provides a clean environment in which to search for BSM physics. Second, final states with Z bosons are predicted in many models of BSM physics, such as supersymmetry (SUSY) [12–16]. For example, the production of a Z boson in the decay $\widetilde{\chi}_2^0 \to \widetilde{\chi}_1^0\,\mathrm{Z}$, where $\widetilde{\chi}_1^0$ ($\widetilde{\chi}_2^0$) is the lightest (second lightest) neutralino, is a direct consequence of the gauge structure of SUSY, and can become a favored channel in regions of the SUSY parameter space where the neutralinos have a large Higgsino or neutral Wino component [17–19]. Our search is also motivated by the existence of cosmological cold dark matter [20], which could consist of weakly-interacting massive particles [21] such as the lightest SUSY neutralino in R-parity conserving SUSY models [22]. If produced in pp collisions, these particles would escape detection and yield events with large $E_{\mathrm{T}}^{\mathrm{miss}}$. Finally, we search for BSM physics in events containing hadronic jets. This is motivated by the fact that new, heavy, strongly-interacting particles predicted by many BSM scenarios may be produced with a large cross section and hence be observable in early LHC data, and such particles tend to decay to hadronic jets. These considerations lead us to our target signature consisting of a leptonically-decaying Z boson produced in association with jets and $E_{\mathrm{T}}^{\mathrm{miss}}$.

After selecting events with jets and a $\mathrm{Z} \to \ell^+\ell^-$ ($\ell = \mathrm{e}, \mu$) candidate, the dominant background consists of SM Z production accompanied by jets from initial-state radiation ($\mathrm{Z} + \text{jets}$). The $E_{\mathrm{T}}^{\mathrm{miss}}$ in $\mathrm{Z} + \text{jets}$ events arises primarily when jet energies are mismeasured. The $\mathrm{Z} + \text{jets}$ cross section is several orders of magnitude larger than our signal, and the artificial $E_{\mathrm{T}}^{\mathrm{miss}}$ is not necessarily well reproduced in simulation. Therefore, the critical prerequisite to a discovery of BSM physics in the $\mathrm{Z} + \text{jets} + E_{\mathrm{T}}^{\mathrm{miss}}$ final state is to establish that a potential excess is not due to SM $\mathrm{Z} + \text{jets}$ production accompanied by artificial $E_{\mathrm{T}}^{\mathrm{miss}}$ from jet mismeasurements. In this paper, we pursue two complementary strategies, denoted the Jet-Z Balance (JZB) and $E_{\mathrm{T}}^{\mathrm{miss}}$ template (MET) methods, which rely on different techniques to suppress the SM $\mathrm{Z} + \text{jets}$ contribution and estimate the remaining background. The two methods employ different search regions, as well as different requirements on the jet multiplicity and Z boson identification. After suppressing the $\mathrm{Z} + \text{jets}$ contribution, the most significant remaining SM background consists of events with a pair of top quarks that both decay leptonically (dilepton $\mathrm{t\bar{t}}$). We exploit the fact that in dilepton $\mathrm{t\bar{t}}$ events the two lepton flavors are uncorrelated, which allows us to use a control sample of $\mathrm{e}\mu$ events, as well as events in the sideband of the dilepton mass distribution, to estimate this background.

The JZB method is sensitive to BSM models where the Z boson and dark matter candidate are the decay products of a heavier particle. In such models, the Z boson and $E_{\mathrm{T}}^{\mathrm{miss}}$ directions are correlated, with the strength of this correlation dependent on the BSM mass spectrum. The $\mathrm{Z}+$jets background contribution to the JZB signal region is estimated from a $\mathrm{Z}+$jets sample, by exploiting the lack of correlation between the direction of the Z boson and $E_{\mathrm{T}}^{\mathrm{miss}}$ in these events for large jet multiplicity. With this method, the significance of an excess is reduced in models where the $E_{\mathrm{T}}^{\mathrm{miss}}$ and Z directions are not correlated.

The MET method relies on two data control samples, one consisting of events with photons accompanied by jets from initial-state radiation ($\gamma+$jets) and one consisting of QCD multijet events, to evaluate the $\mathrm{Z}+$jets background in a high $E_{\mathrm{T}}^{\mathrm{miss}}$ signal region. In contrast to the JZB method, the MET method does not presume a particular mechanism for the production of the Z boson and $E_{\mathrm{T}}^{\mathrm{miss}}$. The significance of an excess is reduced in models that also lead to an excess in both the jets $+ E_{\mathrm{T}}^{\mathrm{miss}}$ and $\gamma+$ jets $+ E_{\mathrm{T}}^{\mathrm{miss}}$ final states.

The paper is organized as follows: we first describe the detector (Section 2), and the data and simulated samples and event selection that are common to both strategies (Section 3). The two methods are then described and the results presented (Sections 4 and 5). Systematic uncertainties on the signal acceptance and efficiency are presented in Section 6. Next, the two sets of results are interpreted in the context of simplified model spectra (SMS) [23–25], which represent decay chains of new particles that may occur in a wide variety of BSM physics scenarios, including SUSY (Section 7). We provide additional information to allow our results to be applied to arbitrary BSM physics scenarios (Section 8). The results are summarized in Section 9.

2 The CMS Detector

The central feature of the CMS apparatus is a superconducting solenoid of 6 m internal diameter, providing a field of 3.8 T. Within the field volume are the silicon pixel and strip tracker, the crystal electromagnetic calorimeter, and the brass/scintillator hadron calorimeter. Muons are measured in gas-ionization detectors embedded in the steel return yoke. In addition to the barrel and endcap detectors, CMS has extensive forward calorimetry. The CMS coordinate system is defined with the origin at the center of the detector and the z axis along the direction of the counterclockwise beam. The transverse plane is perpendicular to the beam axis, with ϕ the azimuthal angle, θ the polar angle, and $\eta = -\ln[\tan(\theta/2)]$ the pseudorapidity. Muons are measured in the range $|\eta| < 2.4$. The inner tracker measures charged particles within the range $|\eta| < 2.5$. A more detailed description of the CMS detector can be found elsewhere [26].

3 Samples and Event Selection

Events are required to satisfy at least one of a set of ee, eμ or $\mu\mu$ double-lepton triggers, with lepton transverse momentum (p_{T}) thresholds of 17 GeV for one lepton and 8 GeV for the other. Events with two oppositely-charged leptons ($\mathrm{e}^+\mathrm{e}^-$, $\mathrm{e}^\pm\mu^\mp$, or $\mu^+\mu^-$) are selected. Details of the lepton reconstruction and identification can be found in Ref. [27] for electrons and in Ref. [28] for muons. Both leptons must have $p_{\mathrm{T}} > 20$ GeV, in the efficiency plateau of the triggers. Electrons (muons) are restricted to $|\eta| < 2.5$ (2.4). For the candidate sample, only $\mathrm{e}^+\mathrm{e}^-$ and $\mu^+\mu^-$ events are used, and the dilepton system is required to have an invariant mass consistent with the mass of the Z boson (m_{Z}). The eμ events are used as a data control sample to estimate the $t\bar{t}$ background.

Because leptons produced in the decays of low-mass particles, such as hadrons containing

b and c quarks, are nearly always inside jets, they can be suppressed by requiring the leptons to be isolated in space from other particles that carry a substantial amount of transverse momentum. The lepton isolation [29] is defined using the scalar sum of both the transverse momentum depositions in the calorimeters and the transverse momenta of tracks in a cone of $\Delta R \equiv \sqrt{(\Delta\eta)^2 + (\Delta\phi)^2} < 0.3$ around each lepton, excluding the lepton itself. Requiring the ratio of this sum to the lepton p_{T} to be smaller than 15% rejects the large background arising from QCD production of jets.

We select jets [30] with $p_{\mathrm{T}} > 30\,\mathrm{GeV}$ and $|\eta| < 3.0$, separated by $\Delta R > 0.4$ from leptons passing the analysis selection. We use the particle flow (PF) method [31] to reconstruct charged and neutral hadrons, muons, electrons, and photons. The PF objects are clustered to form jets using the anti-k_{T} clustering algorithm [32] with a distance parameter of 0.5, as implemented in the FASTJET package [33, 34]. We apply p_{T}- and η-dependent corrections to account for residual effects of non-uniform detector response. The contribution to the jet energy from pile-up is estimated on an event-by-event basis using the jet area method described in Ref. [35], and is subtracted from the overall jet p_{T}. The missing transverse momentum $E_{\mathrm{T}}^{\mathrm{miss}}$ is defined as the magnitude of the vector sum of the transverse momenta of all PF objects. The $E_{\mathrm{T}}^{\mathrm{miss}}$ vector is the negative of that same vector sum.

The sample passing the above preselection requirements is dominated by SM $\mathrm{Z}+$jets events, which must be suppressed in order to achieve sensitivity to BSM physics. As discussed in the introduction, we pursue two complementary approaches to evaluate the $\mathrm{Z}+$jets background. Samples of $\mathrm{Z}+$jets, $\mathrm{t\bar{t}}$, WW, WZ, and ZZ Monte Carlo (MC) simulated events generated with MADGRAPH 5.1.1.0 [36] are used to guide the design of these methods, but the dominant backgrounds are estimated with techniques based on data control samples. Events produced by MADGRAPH are passed to PYTHIA 6.4.22 [37] for the generation of parton showers. Additional MC samples of $\mathrm{Z}+$jets, $\gamma+$jets, and QCD multijet events generated with PYTHIA 6.4.22 are used to validate the $E_{\mathrm{T}}^{\mathrm{miss}}$ template method of Sec. 5. We also present the expected event yields for two benchmark scenarios of the constrained minimal supersymmetric extension of the standard model (CMSSM) [38], denoted LM4 and LM8 [39], which are generated with the same version of PYTHIA. The CMSSM is described with five parameters: the universal scalar and gaugino masses m_0 and $m_{1/2}$, the universal soft SUSY-breaking parameter A_0, the ratio of vacuum expectation values of the two Higgs doublets $\tan\beta$, and the sign of the Higgs mixing parameter μ. The LM4 (LM8) parameter sets are $m_0 = 210\ (500)\,\mathrm{GeV}$, $m_{1/2} = 285\ (300)\,\mathrm{GeV}$, $\tan\beta = 10$, $\mathrm{sign}(\mu) = +$, and $A_0 = 0\ (-300)\,\mathrm{GeV}$. The LM4 scenario is excluded in Ref. [3]; this paper is the first to exclude LM8. In these two scenarios heavy neutralinos predominantly decay to a Z boson and a lighter neutralino. All samples are generated using the CTEQ6 [40] parton distribution functions (PDFs) and normalized to next-to-leading order (NLO) cross sections. Simulation of the CMS detector response is performed using GEANT4 [41]. The simulated events are subsequently reconstructed and analyzed in the same way as the data, and are rescaled to describe the measured distribution of overlapping pp collisions in the same bunch crossing (referred to as "pile-up reweighting").

4 JZB Search

4.1 Jet-Z Balance Variable

The JZB variable is defined in the xy plane as

$$\text{JZB} = \left|\sum_{\text{jets}} \vec{p}_{\text{T}}\right| - \left|\vec{p}_{\text{T}}{}^{(\text{Z})}\right| \approx \left|-\vec{E}_{\text{T}}^{\text{miss}} - \vec{p}_{\text{T}}{}^{(\text{Z})}\right| - \left|\vec{p}_{\text{T}}{}^{(\text{Z})}\right|. \quad (1)$$

Thus JZB measures the imbalance between the p_{T} of the Z boson and that of the hadronic system. In SM $\text{Z}+\text{jets}$ events, the JZB distribution is approximately symmetric about zero, while for BSM physics it may be asymmetric, due to correlated production of the Z boson and invisible particles. Five signal regions are defined by requirements on the JZB event variable, from $\text{JZB} > 50\,\text{GeV}$ to $\text{JZB} > 250\,\text{GeV}$ in steps of 50 GeV. The signal region in the invariant mass distribution is defined as $|m_{\ell\ell} - m_{\text{Z}}| < 20\,\text{GeV}$.

In SM $\text{Z}+\text{jets}$ events, the JZB variable is analogous to $E_{\text{T}}^{\text{miss}}$ with sign information. The sign depends on whether $E_{\text{T}}^{\text{miss}}$ is due to an under- or over-measurement of the jet energy. The probability of a downward fluctuation of the jet energy measurement is in general higher than the probability of an upward fluctuation, leading to an asymmetry of the JZB distribution in SM Z events with exactly 1 jet. However, the JZB distribution in SM $\text{Z}+\text{jets}$ events becomes more Gaussian with increasing jet multiplicity, because in multijet events the direction of a mismeasured jet is uncorrelated with the direction of the Z boson. Already in three-jet events, where in the most probable configuration, the two leading jets are back-to-back [42], instrumental effects largely cancel. For this reason the JZB method focuses on events containing at least three jets.

We search for BSM events where the Z boson is the decay product of a heavier (parent) particle of mass m_M and is produced in conjunction with an undetectable decay product of mass m_{χ}, which gives rise to $E_{\text{T}}^{\text{miss}}$. Let p^* be the characteristic momentum of the decay products in the rest frame of the parent particle. If the parent particle has a mass of the order of the electroweak scale, $m_M \sim O(m_{\chi} + m_{\text{Z}})$, p^* is small, and p^* can be smaller than the laboratory momentum of the parent. In that case, the daughter particles all appear in a tightly collimated angular region, the transverse momenta of the Z and invisible particle are balanced by the other particles in the decay chain, and large values of JZB can ensue. An example of such a decay chain is $\tilde{\text{g}} \to \bar{\text{q}} + \tilde{\text{q}} \to \bar{\text{q}} + \text{q} + \tilde{\chi}_2^0 \to \bar{\text{q}} + \text{q} + \text{Z} + \tilde{\chi}_1^0$, where $\tilde{\text{g}}$, $\tilde{\text{q}}$, and $\tilde{\chi}_{1,2}^0$ are the gluino, squark, and neutralino supersymmetric particles.

The signal and background discrimination arising from the angular correlation between the Z boson and $E_{\text{T}}^{\text{miss}}$ can be reduced in certain circumstances. For example, in R-parity-conserving SUSY, supersymmetric particles are produced in pairs and there are two decay chains with one undetected lightest stable particle (LSP) at the end of each chain. It can happen that the two unobserved particle momenta cancel each other, leading to small $E_{\text{T}}^{\text{miss}}$ and JZB values. Such configurations are, however, disfavored by the selection of events with significant $E_{\text{T}}^{\text{miss}}$, or large JZB, which is equivalent to requiring that the two LSPs do not balance. The angular correlation is therefore preserved in events with significant $E_{\text{T}}^{\text{miss}}$.

To summarize, the balance between the jet system and the $\text{Z} + E_{\text{T}}^{\text{miss}}$ system leads to large, positive JZB in events where $E_{\text{T}}^{\text{miss}}$ and the Z boson are pair-produced, while the $\text{JZB} > 0$ and $\text{JZB} < 0$ regions are evenly populated in SM $\text{Z}+\text{jets}$ events.

4.2 Background Determination

The principal SM backgrounds are divided in two categories. Backgrounds that produce opposite-flavor (OF) pairs $(\text{e}^+\mu^-, \text{e}^-\mu^+)$ as often as same-flavor (SF) pairs $(\text{e}^+\text{e}^-, \mu^+\mu^-)$ are referred to as "flavor–symmetric backgrounds". This category is dominated by $\text{t}\bar{\text{t}}$ processes. Backgrounds with two SF leptons from a Z boson are referred to as "Z boson backgrounds". This category is dominated by SM $\text{Z}+\text{jets}$ production.

Three non-overlapping data control regions are used to predict the contribution of flavor-symmetric backgrounds: (a) OF events compatible with the Z boson mass hypothesis (referred to as "Z-peak region"), (b) OF events in the sideband of the Z boson mass peak, and (c) SF events in this sideband. The sideband region is defined as the union of $55 < m_{\ell\ell} < 70\,\text{GeV}$ and $112 < m_{\ell\ell} < 160\,\text{GeV}$; it is chosen so that it includes the same number of events as the Z-peak region in $\mathrm{t\bar{t}}$ simulation. The two OF data control samples are compared in the region $30\,\text{GeV} < |\text{JZB}| < 50\,\text{GeV}$, which is outside the signal regions and has little contribution from signal or $\text{Z}(\rightarrow \tau\tau) + \text{jets}$. The event yields from the two data control samples in this region are found to be in good agreement with each other and with expectations from the MC simulation. The systematic uncertainties on the number of events estimated from the three data control regions are assessed using a large sample of simulated $\mathrm{t\bar{t}}$ events. The JZB distribution in the SF Z-peak (signal) region is found to agree well with the corresponding distributions in the three control regions. A 25% uncertainty is assigned to each individual estimate in order to cover discrepancies at large JZB values, where the number of MC events is low, as well as small differences between the data and MC simulation in the shape of the JZB distribution.

The total contribution from flavor-symmetric backgrounds in the signal region is computed as the average of the yields in the three data control regions, as they provide independent estimates of the same background process. The systematic uncertainties assigned to these yields are approximately uncorrelated, and hence are added quadratically. The absence of strong correlation is confirmed in MC simulation, as well as from the aforementioned comparison of the number of events in the $30\,\text{GeV} < |\text{JZB}| < 50\,\text{GeV}$ region.

SM backgrounds with a reconstructed Z boson are estimated using the negative JZB region after subtraction of flavor-symmetric backgrounds. This procedure relies on the fact that $\text{Z} + \text{jets}$ events with three or more jets evenly populate the negative and positive sides of the JZB distribution, as described above. The method is validated using a large sample of simulated $\text{Z} + \text{jets}$ events and the JZB distributions in the negative and positive JZB regions are found to agree very well. We assign a 25% systematic uncertainty to the corresponding prediction in order to cover small differences between the data and MC simulation in the shape of the JZB distribution.

Other backgrounds, though less significant, are also accounted for in these estimates. Contributions from the SM WZ and ZZ processes are incorporated into the $\text{Z} + \text{jets}$ estimate, since in these events the $E_{\text{T}}^{\text{miss}}$ and the Z boson candidates do not share the same parent particle. The background estimate from OF pairs accounts for WW, $\text{Z} \rightarrow \tau\tau$, and single-top production. Finally, events with one or more jets reconstructed as electrons or non-isolated leptons (from QCD multijet, $\gamma + \text{jets}$, or electroweak processes) are accounted for by the background estimate from the sideband control regions.

The overall background prediction method is validated using a simulated sample including all SM backgrounds, with and without the inclusion of LM4 signal events. The comparison between the true and predicted distributions is shown in Fig. 1 for the two cases. The inclusion of LM4 signal slightly modifies the predicted distribution because of contribution from the signal to the control regions. The slope change around $\text{JZB} = 50\,\text{GeV}$ corresponds to the region where the $\mathrm{t\bar{t}}$ background starts to dominate. The integrated event yields for the various signal regions are summarized in Table 1. We find that there is good agreement in the background-only case, while good sensitivity to a possible signal remains.

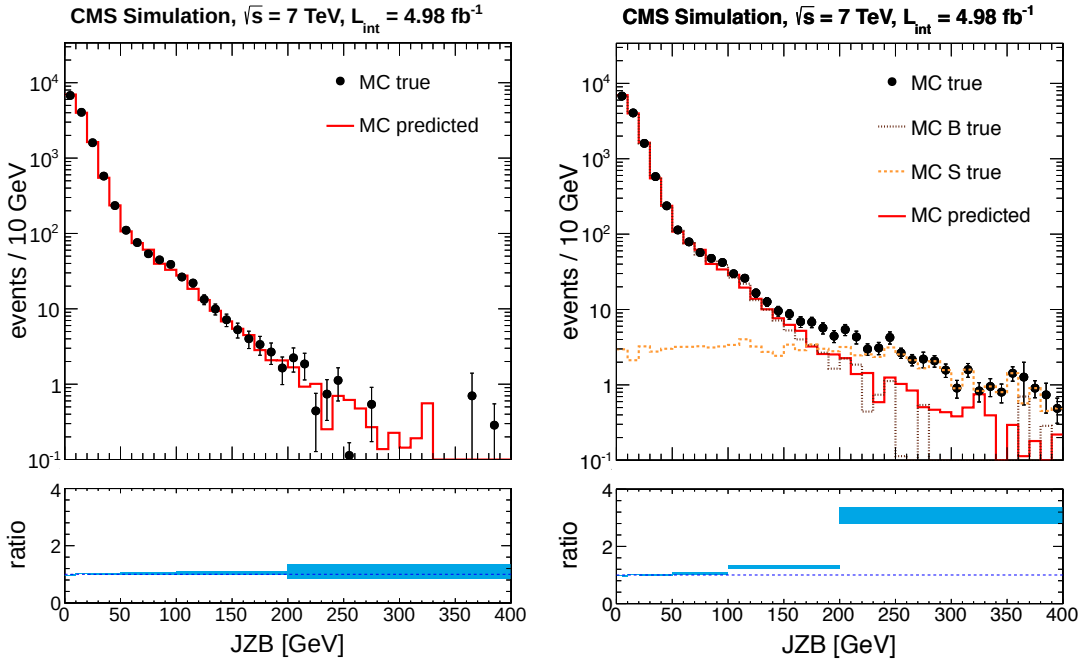

Figure 1: Comparison between true and predicted JZB distributions in simulated samples for the background-only (left) and LM4-plus-background (right) hypotheses. "MC B" and "MC S" denote the background and signal contributions to the true distribution, respectively. The lower plots show the ratio between true and predicted distributions. The error bars on the true distribution and in the ratio indicate the statistical uncertainty only.

Table 1: Comparison between true and predicted JZB event yields in SM MC simulation for the various signal regions. Uncertainties on the true MC yields reflect the limited MC statistics. The first (second) uncertainty in the MC predicted yields indicates the statistical (systematic) component.

Region	MC true	MC predicted
JZB $>$ 50 GeV	420 ± 11	$414 \pm 16 \pm 59$
JZB $>$ 100 GeV	102 ± 5	$98 \pm 6 \pm 14$
JZB $>$ 150 GeV	25 ± 2.6	$24 \pm 3.4 \pm 3.0$
JZB $>$ 200 GeV	8.5 ± 1.6	$7.8 \pm 1.8 \pm 1.1$
JZB $>$ 250 GeV	2.2 ± 0.9	$3.2 \pm 1.2 \pm 0.5$

4.3 Results

The comparison between the observed and predicted distributions is shown in Fig. 2. The observed and predicted yields in the signal regions are summarized in Table 2, along with 95% confidence level (CL) upper limits on the yields of any non-SM process. Upper limits are computed throughout this paper using a modified frequentist method (CL_S) [43, 44]. The nuisance parameters (described in Section 6) are modeled with a lognormal distribution. Table 2 also shows the LM4 and LM8 yields, determined using NLO production cross sections. These yields are corrected to account for the contribution of signal to the background control regions, which tends to suppress the apparent yield of signal in the signal region. The correction is performed by subjecting the signal samples to the same procedures as the data and subtracting the resulting prediction from the signal yield in the signal region. The expected LM4 and LM8 yields exceed the upper limits on the non-SM contributions to the yields in the high JZB signal regions.

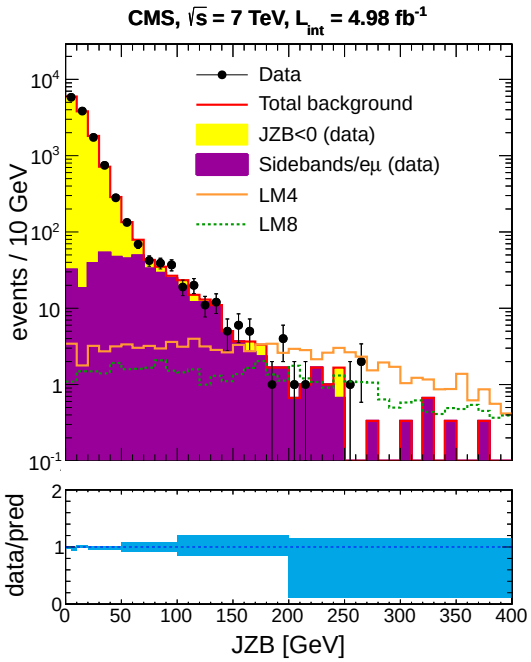

Figure 2: Comparison between the measured JZB distribution in the JZB > 0 region and that predicted from data control samples. The distribution from the LM4 MC is overlaid. The bottom plot shows the ratio between the observed and predicted distributions. The error bars indicate the statistical uncertainties in data only.

5 MET Search

For the MET method, we select events with two or more jets. Compared to the JZB method, the dilepton mass requirement is tightened to $|m_{\ell\ell} - m_Z| < 10\,\text{GeV}$, in order to further constrain mismeasurements of the lepton p_T's and to suppress the $t\bar{t}$ background. As in the JZB method, the principal background is $Z +$ jets events. To suppress this background, we require the events to have large E_T^{miss}. Specifically, we define three signal regions:

- $E_T^{miss} > 100\,\text{GeV}$ (loose signal region);
- $E_T^{miss} > 200\,\text{GeV}$ (medium signal region);

Table 2: Total number of events observed in the JZB signal regions and corresponding background predictions from data control regions. The first uncertainty is statistical and the second systematic. For the observed yields, the first (second) number in parentheses is the yield in the e^+e^- ($\mu^+\mu^-$) final state. The 95% CL upper limit (UL) on non-SM yields and the NLO yields for the LM4 and LM8 benchmark SUSY scenarios are also given, including the systematic uncertainties and the correction for signal contribution to the background control regions (see text for details).

	JZB $>$ 50 GeV	100 GeV	150 GeV	200 GeV	250 GeV
Z bkg	$97 \pm 13 \pm 38$	$8 \pm 3 \pm 3$	$2.7 \pm 1.8 \pm 0.8$	$1.0 \pm 1.0 \pm 0.3$	0
Flavor-symmetric	$311 \pm 10 \pm 45$	$81 \pm 5 \pm 12$	$19 \pm 3 \pm 3$	$7 \pm 2 \pm 1$	$2.0 \pm 0.8 \pm 0.3$
Total bkg	$408 \pm 16 \pm 59$	$89 \pm 6 \pm 12$	$22 \pm 3 \pm 3$	$8 \pm 2 \pm 1$	$2.0 \pm 0.8 \pm 0.3$
Data	408 (203,205)	88 (52,36)	21 (13,8)	5 (3,2)	3 (2,1)
Observed UL	114	32	14	6	6
Expected UL	111	31	13	7	4
LM4	62 ± 4	52 ± 4	40 ± 4	29 ± 4	18 ± 4
LM8	23 ± 2	19 ± 2	16 ± 2	11.4 ± 1.7	7.8 ± 1.5

- $E_T^{miss} > 300$ GeV (tight signal region).

The use of multiple signal regions allows us to be sensitive to BSM physics with differing E_T^{miss} distributions. To estimate the residual Z + jets background with E_T^{miss} from jet mismeasurements, we model the E_T^{miss} in Z + jets events using γ + jets and QCD control samples in data. After applying the E_T^{miss} requirement, the dominant background is expected to be $t\bar{t}$ in all three signal regions. This background is estimated from a control sample of $e\mu$ events in data. Additional sub-leading backgrounds from WZ and ZZ diboson production are estimated from simulation.

5.1 Background Estimates

5.1.1 Z + jets Background Estimate

The background from SM Z + jets production is estimated using a E_T^{miss} template method [45]. In Z + jets events, the E_T^{miss} is dominated by mismeasurements of the hadronic system. Therefore, the E_T^{miss} distribution in these events can be modeled using a control sample with no true E_T^{miss} and a similar hadronic system as in Z + jets events. We use two complementary control samples: one consisting of γ + jets events and one consisting of QCD multijet events. The γ + jets (QCD multijet) events are selected with a set of single photon (single jet) triggers with online p_T tresholds varying from 20–90 GeV (30–370 GeV). To account for kinematic differences between the hadronic systems in the control and signal samples, the expected E_T^{miss} distribution of a Z + jets event is obtained from the E_T^{miss} distribution of γ + jets or QCD multijet events of the same jet multiplicity and scalar sum of jet transverse energies, normalized to unit area; these normalized distributions are referred to as E_T^{miss} templates. The two control samples are complementary. The γ + jets events have a topology that is similar to the Z + jets events, since both consist of a well-measured object recoiling against a system of hadronic jets. When selecting photons, we include hadronic jets in which a large fraction of the energy is carried by photons or neutral pions. Such jets are well measured; the E_T^{miss} in these events arises from jets with a large hadronic energy fraction as in the true γ + jets events. The QCD multijet sample has better statistical precision due to the larger number of events, and eliminates possible contribu-

tions to $E_{\mathrm{T}}^{\mathrm{miss}}$ from mismeasurement of the photon in the γ + jets sample. The $E_{\mathrm{T}}^{\mathrm{miss}}$ templates extracted from the QCD sample must be corrected for a small bias of the $E_{\mathrm{T}}^{\mathrm{miss}}$, which is observed in γ + jets and Z + jets events in the direction of the recoiling hadronic system, due to a small systematic under-measurement of the jet energies. This bias of the $E_{\mathrm{T}}^{\mathrm{miss}}$ is measured to be approximately 6% of the p_{T} of the hadronic recoil system, and the correction primarily affects the bulk of the $E_{\mathrm{T}}^{\mathrm{miss}}$ distribution. A similar effect is present when using the γ + jets templates because a minimum p_{T} threshold is applied to the photons but not to the Z bosons. However, the maximum resulting bias in the $E_{\mathrm{T}}^{\mathrm{miss}}$ is approximately 1 GeV, and is hence negligible.

Because jets in QCD dijet events have a different topology than those in Z + 2 jet events, the γ + jets method alone is used to determine the Z + jets background for events with exactly two jets. For events with at least three jets, we use the average of the background estimates from the γ + jets and QCD multijets methods. The two methods yield consistent predictions for events with at least three jets, which illustrates the robustness of the $E_{\mathrm{T}}^{\mathrm{miss}}$ template method and provides a cross-check of the data-driven background prediction. For the benchmark SUSY scenarios LM4 and LM8, we have verified that the impact of signal contamination on the predicted background from the $E_{\mathrm{T}}^{\mathrm{miss}}$ template method is negligible.

The systematic uncertainty in the background prediction from the γ + jets method is dominated by possible differences between the predicted and true number of events when we apply the background estimate to the MC, which is limited by the statistical precision of the MC samples (MC closure test, 30% uncertainty). Additional uncertainties are evaluated by varying the photon selection criteria (10% uncertainty) and from the difference in the number of reconstructed pile-up interactions in the Z + jets and γ + jets samples (5% uncertainty). The total uncertainty is 32%. The corresponding uncertainty in the background prediction from the QCD multijet method is dominated by possible differences between the predicted and true number of events in the MC closure test (ranging from 20% for $E_{\mathrm{T}}^{\mathrm{miss}} > 30$ GeV to 100% for $E_{\mathrm{T}}^{\mathrm{miss}} > 100$ GeV). The uncertainty in the bias of the $E_{\mathrm{T}}^{\mathrm{miss}}$ in the direction of the hadronic recoil contributes an additional 16% uncertainty to this background prediction.

5.1.2 Opposite-Flavor Background Estimate

As in the JZB method, the $\mathrm{t\bar{t}}$ contribution is estimated using an OF subtraction technique, based on the equality of the $\mathrm{t\bar{t}}$ yield in the OF and SF final states after correcting for the differences in the e and μ selection efficiencies. Other backgrounds for which the lepton flavors are uncorrelated (for example, $\mathrm{W^+W^-}$, $\gamma^*/\mathrm{Z} \to \tau^+\tau^-$ and single-top processes, which are dominated by the tW production mechanism) are also included in this estimate.

To predict the SF yield in the $E_{\mathrm{T}}^{\mathrm{miss}}$ signal regions, we use the OF yield satisfying the same $E_{\mathrm{T}}^{\mathrm{miss}}$ requirements. This yield is corrected using the ratio of selection efficiencies $R_{\mu\mathrm{e}} \equiv \varepsilon_\mu/\varepsilon_e = 1.07 \pm 0.07$, which is evaluated from studies of $\mathrm{Z} \to \mu^+\mu^-$ and $\mathrm{Z} \to \mathrm{e^+e^-}$ events in data. The uncertainty on this quantity takes into account a small variation with respect to lepton p_{T}. To improve the statistical precision of the background estimate, we do not require the OF events to lie in the Z mass region, and we apply a scale factor $K = 0.16 \pm 0.01$, extracted from simulation, to account for the fraction of $\mathrm{t\bar{t}}$ events that satisfy $|m_{\ell\ell} - m_{\mathrm{Z}}| < 10$ GeV. The uncertainty in K is determined by the difference between this quantity evaluated in data versus simulation. An alternate method is to use OF events in the Z mass window; scaling is not required, but fewer events are available. This method yields a prediction that is consistent with that from the nominal method but with a larger statistical uncertainty. The systematic uncertainty on the OF background prediction is dominated by a 25% uncertainty in the yield predicted for the $E_{\mathrm{T}}^{\mathrm{miss}} > 200$ GeV region, due to possible differences between the true and predicted number of

events in MC closure tests. The uncertainties in the correction factors $R_{\mu e}$ (7%) and K (6%) also contribute.

5.1.3 Other Backgrounds

Backgrounds from pairs of WZ and ZZ vector bosons are estimated from MC, and a 50% systematic uncertainty is assessed based on comparison of simulation to data in events with jets and exactly 3 leptons (WZ control sample, MC expected purity approximately 90%) and exactly 4 leptons (ZZ control sample, MC expected purity approximately 100%), which have limited statistical precision due to small event yields. Backgrounds from events with misidentified leptons are negligible due to the requirement of two isolated leptons with $p_{\mathrm{T}} > 20\,\mathrm{GeV}$ in the Z mass window.

5.2 Results

The data and SM predictions are shown in Fig. 3 and summarized in Table 3 ($N_{\mathrm{jets}} \geq 2$) and Table 4 ($N_{\mathrm{jets}} \geq 3$). In addition to the loose, medium, and tight signal regions defined above, we quote the predicted and observed event yields in two low $E_{\mathrm{T}}^{\mathrm{miss}}$ regions, which allows us to validate our background estimates with increased statistical precision. For all five regions, the observed yields are consistent with the predicted background yields. No evidence for BSM physics is observed. We place 95% CL upper limits on the non-SM contributions to the yields in the signal regions. These model-independent upper limits may be used in conjunction with the signal efficiency model discussed in Section 8 to perform exclusions in the context of an arbitrary BSM physics model. We quote results separately for $N_{\mathrm{jets}} \geq 2$ and $N_{\mathrm{jets}} \geq 3$ to improve the sensitivity to BSM models with low and high average jet multiplicities, respectively. We also quote the NLO expected yields for the SUSY benchmark processes LM4 and LM8, including the statistical component and the systematic uncertainties discussed in Sec. 6. To account for the impact of signal contamination, we correct the LM4 and LM8 yields by subtracting the expected increase in the OF background estimate that would occur if these signals were present in the data. As mentioned above, the contribution from LM4 and LM8 to the $E_{\mathrm{T}}^{\mathrm{miss}}$ template background estimate is negligible. The expected LM4 and LM8 yields exceed the upper limits on the non-SM contributions to the yields in those signal regions with a minimum $E_{\mathrm{T}}^{\mathrm{miss}}$ requirement of 200 GeV.

6 Signal Acceptance and Efficiency Uncertainties

The acceptance and efficiency, as well as the systematic uncertainties on these quantities, depend on the signal model under consideration. For some of the individual uncertainties, we quote values based on SM control samples with kinematic properties similar to the SUSY benchmark models. For others that depend strongly on the kinematic properties of the event, the systematic uncertainties are quoted model-by-model and separately for the various signal regions.

The systematic uncertainty on the lepton acceptance consists of two parts: the trigger efficiency uncertainty and the identification and isolation uncertainty. The trigger efficiency for two leptons of $p_{\mathrm{T}} > 20\,\mathrm{GeV}$ is measured in a $\mathrm{Z} \to \ell\ell$ data sample, with an uncertainty of 2%. We verify that the simulation reproduces the lepton identification and isolation efficiencies in data using $\mathrm{Z} \to \ell\ell$ samples, within a systematic uncertainty of 2% per lepton.

Another significant source of systematic uncertainty in the acceptance is associated with the jet and $E_{\mathrm{T}}^{\mathrm{miss}}$ energy scale. The impact of this uncertainty depends on the final state under

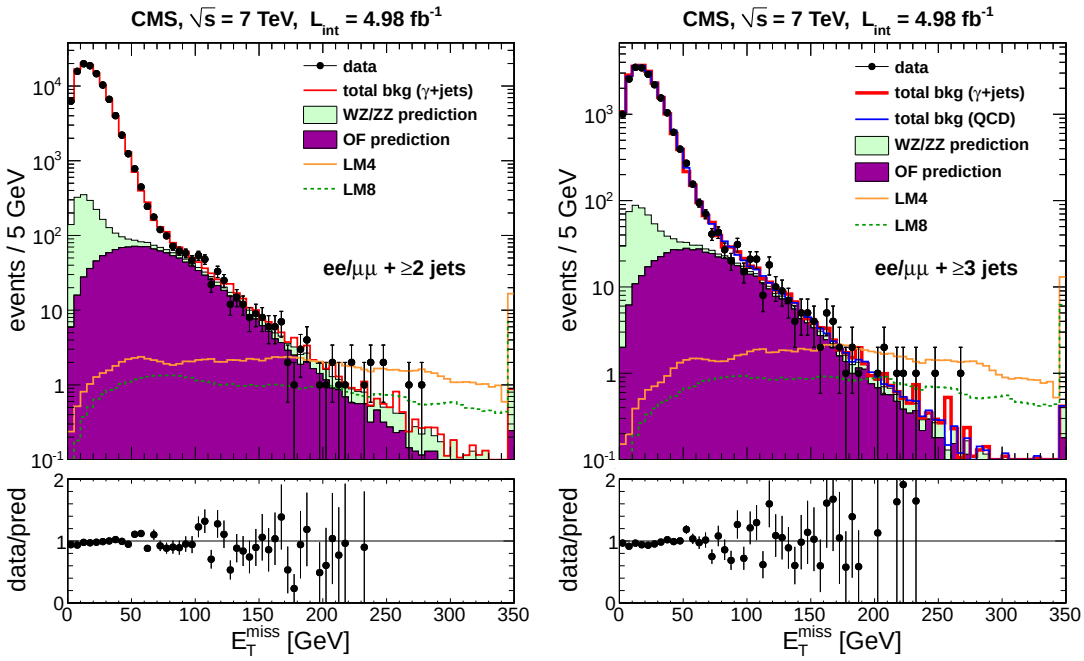

Figure 3: The observed $E_{\mathrm{T}}^{\mathrm{miss}}$ distribution for events with $N_{\mathrm{jets}} \geq 2$ (left) and $N_{\mathrm{jets}} \geq 3$ (right) for data (black points), predicted OF background from simulation normalized to the eμ yield in data (solid dark purple histogram), WZ + ZZ background (solid light green histogram), and total background including the Z + jets predicted from γ + jets (red line) and QCD (blue line) $E_{\mathrm{T}}^{\mathrm{miss}}$ templates. The ratio of the observed and total predicted yields (data/pred) is indicated in the bottom plots using the γ + jets (left) and average of the γ + jets and QCD (right) methods. The error bars indicate the statistical uncertainties in data only.

Table 3: Summary of results in the regions $E_{\mathrm{T}}^{\mathrm{miss}} > 30$, 60, 100, 200, and 300 GeV for $N_{\mathrm{jets}} \geq 2$. The total predicted background (total bkg) is the sum of the Z + jets background predicted from the γ + jets $E_{\mathrm{T}}^{\mathrm{miss}}$ template method (Z bkg), the background predicted from OF events (OF bkg), and the WZ + ZZ background predicted from simulation (VZ bkg). The first (second) uncertainty indicates the statistical (systematic) component. For the observed yield (data), the first (second) number in parentheses is the yield in the ee ($\mu\mu$) final state. The 95% CL observed and expected upper limits (UL) on the non-SM yield are indicated. The expected NLO yields for the LM4 and LM8 benchmark SUSY scenarios are also given, including the systematic uncertainties and the correction for the impact of signal contamination indicated in the text.

	$E_{\mathrm{T}}^{\mathrm{miss}} > 30$ GeV	$E_{\mathrm{T}}^{\mathrm{miss}} > 60$ GeV	$E_{\mathrm{T}}^{\mathrm{miss}} > 100$ GeV	$E_{\mathrm{T}}^{\mathrm{miss}} > 200$ GeV	$E_{\mathrm{T}}^{\mathrm{miss}} > 300$ GeV
Z bkg	$15070 \pm 161 \pm 4822$	$484 \pm 23 \pm 155$	$36 \pm 4.6 \pm 11$	$2.4 \pm 0.6 \pm 0.8$	$0.4 \pm 0.2 \pm 0.1$
OF bkg	$1116 \pm 13 \pm 100$	$680 \pm 10 \pm 61$	$227 \pm 6.0 \pm 20$	$11 \pm 1.3 \pm 3.1$	$1.6 \pm 0.5 \pm 0.4$
VZ bkg	$269 \pm 0.9 \pm 135$	$84 \pm 1.0 \pm 42$	$35 \pm 0.5 \pm 17$	$5.3 \pm 0.4 \pm 2.7$	$1.2 \pm 0.4 \pm 0.6$
Total bkg	$16455 \pm 161 \pm 4825$	$1249 \pm 25 \pm 172$	$297 \pm 7.5 \pm 29$	$19 \pm 1.5 \pm 4.1$	$3.2 \pm 0.7 \pm 0.7$
Data	16483 (8243,8240)	1169 (615,554)	290 (142,148)	14 (8,6)	0
Observed UL	9504	300	57	8.3	3.0
Expected UL	9478	349	60	11	4.6
LM4	120 ± 7.0	108 ± 6.7	93 ± 6.6	53 ± 7.3	24 ± 6.2
LM8	52 ± 3.2	46 ± 3.0	37 ± 2.8	21 ± 2.8	9.1 ± 2.3

Table 4: Summary of results for $N_{\text{jets}} \geq 3$. The details are the same as for the $N_{\text{jets}} \geq 2$ results quoted in Table 3, except that the total background prediction is based on the average of the background predictions from the QCD and $\gamma +$ jets template methods, which are quoted separately.

	$E_{\text{T}}^{\text{miss}} > 30\,\text{GeV}$	$E_{\text{T}}^{\text{miss}} > 60\,\text{GeV}$	$E_{\text{T}}^{\text{miss}} > 100\,\text{GeV}$	$E_{\text{T}}^{\text{miss}} > 200\,\text{GeV}$	$E_{\text{T}}^{\text{miss}} > 300\,\text{GeV}$
Z bkg (QCD)	$4010 \pm 65 \pm 800$	$191 \pm 12 \pm 56$	$11 \pm 0.7 \pm 11$	$0.7 \pm 0.05 \pm 0.7$	$0.1 \pm 0.02 \pm 0.1$
Z bkg ($\gamma +$ jets)	$3906 \pm 61 \pm 1250$	$187 \pm 10 \pm 60$	$14 \pm 1.7 \pm 4.6$	$1.7 \pm 0.5 \pm 0.5$	$0.3 \pm 0.2 \pm 0.1$
OF bkg	$442 \pm 8.0 \pm 40$	$284 \pm 7.0 \pm 26$	$107 \pm 4.1 \pm 10$	$7.5 \pm 1.1 \pm 2.0$	$1.1 \pm 0.4 \pm 0.3$
WZ bkg	$86 \pm 1.0 \pm 43$	$26 \pm 0.3 \pm 13$	$11 \pm 0.2 \pm 5.6$	$1.9 \pm 0.2 \pm 1.0$	$0.4 \pm 0.2 \pm 0.2$
Total bkg (QCD)	$4539 \pm 66 \pm 802$	$502 \pm 14 \pm 63$	$129 \pm 4.2 \pm 16$	$10 \pm 1.1 \pm 2.3$	$1.6 \pm 0.4 \pm 0.4$
Total bkg ($\gamma +$ jets)	$4435 \pm 62 \pm 1251$	$498 \pm 12 \pm 66$	$132 \pm 4.4 \pm 12$	$11 \pm 1.2 \pm 2.2$	$1.9 \pm 0.5 \pm 0.4$
Total bkg (average)	$4487 \pm 64 \pm 1027$	$500 \pm 13 \pm 65$	$131 \pm 4.3 \pm 14$	$11 \pm 1.2 \pm 2.3$	$1.8 \pm 0.5 \pm 0.4$
Data	4501 (2272,2229)	479 (267,212)	137 (73,64)	8 (3,5)	0
Observed UL	2028	120	40	6.7	3.0
Expected UL	2017	134	36	8.4	3.9
LM4	97 ± 6.1	90 ± 6.1	79 ± 6.6	44 ± 7.1	19 ± 5.4
LM8	42 ± 2.6	39 ± 2.5	33 ± 2.5	19 ± 2.7	8.3 ± 2.1

consideration. Final states characterized by very large $E_{\text{T}}^{\text{miss}}$ are less sensitive to this uncertainty than those with $E_{\text{T}}^{\text{miss}}$ values near the minimum signal region requirements. To estimate this uncertainty, we have used the method of Ref. [29] to evaluate the systematic uncertainties in the acceptance for the two benchmark SUSY points. The energies of jets in this analysis are known to 7.5% (not all the corrections in Ref. [30] were applied). For LM4 and LM8, the corresponding systematic uncertainties on the signal region yields vary from 4–6% for $E_{\text{T}}^{\text{miss}} > 100\,\text{GeV}$ to 24–28% for $E_{\text{T}}^{\text{miss}} > 300\,\text{GeV}$.

The impact of the hadronic scale uncertainty on the JZB efficiency is estimated by varying the jet energy scale by one standard deviation [30]. This leads to a systematic uncertainty of 3–6% on the signal efficiency, depending on the model and the signal region. The JZB scale is then varied by 5% to account for the uncertainty in unclustered energy deposits. The corresponding signal efficiency uncertainties vary between 1% (JZB $> 50\,\text{GeV}$) and 7% (JZB $> 250\,\text{GeV}$) for LM4, and between 1% and 10% for LM8.

Uncertainties on the PDFs are determined individually for each scenario and are propagated to the efficiency, as recommended in Ref. [46]. The uncertainty associated with the integrated luminosity is 2.2% [47].

7 Interpretation

In the absence of a significant excess, we set upper limits on the production cross section of SMS models [23–25], which represent decay chains of new particles that may occur in a wide variety of BSM physics scenarios, including SUSY. We provide the signal selection efficiencies in the model parameter space. These efficiencies may be employed to validate and calibrate the results of fast simulation software used to determine the signal efficiency of an arbitrary BSM model. This allows our results to be applied to BSM models beyond those examined in this paper. We also provide cross section upper limits in the parameter space of these models, and exclude a region of the parameter space assuming reference cross sections and a 100% branching fraction to the final state under consideration (the Z boson is allowed to decay according to the well-known SM branching fractions).

Figure 4 illustrates the process considered in this study: two gluinos are produced, each of

which decays to a pair of jets and the second-lightest neutralino $\widetilde{\chi}_2^0$, which itself decays to a Z boson and the LSP $\widetilde{\chi}_1^0$. The parameters of the model are the masses of the gluino ($m_{\widetilde{g}}$) and of the LSP ($m_{\widetilde{\chi}_1^0}$). The mass of the intermediate neutralino ($m_{\widetilde{\chi}_2^0}$) is fixed to $m_{\widetilde{\chi}_2^0} = m_{\widetilde{\chi}_1^0} + x \cdot (m_{\widetilde{g}} - m_{\widetilde{\chi}_1^0})$, with $x = 0.5$. The results are only presented in the region where the particle masses as specified above satisfy $m_{\widetilde{\chi}_2^0} > m_{\widetilde{\chi}_1^0} + m_Z$. Additional interpretations for a different choice of x as well as for a model inspired by gauge-mediated SUSY breaking are included in the supplementary materials of this paper.

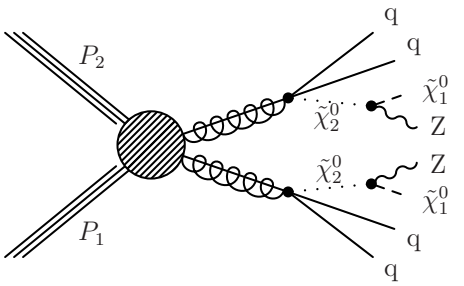

Figure 4: Simplified model for the production of two gluinos decaying into two Z bosons, two $\widetilde{\chi}_1^0$ particles, and jets.

For the JZB analysis, we calculate the observed and expected upper limits on the cross section using the results in all signal regions, and select the observed limit corresponding to the best expected limit for each parameter point. For the MET analysis, the cross section upper limit is based on simultaneous counting experiments in the three exclusive regions of $100\,\text{GeV} < E_\text{T}^\text{miss} < 200\,\text{GeV}$, $200\,\text{GeV} < E_\text{T}^\text{miss} < 300\,\text{GeV}$, and $E_\text{T}^\text{miss} > 300\,\text{GeV}$, as summarized in Table 5, since this exclusive binning improves the sensitivity to a specific BSM model. The model-dependent systematic uncertainties (energy scale and PDF uncertainties) are determined for each point. To interpret these limits in terms of the gluino pair-production cross section, we use a reference cross section $\sigma^\text{NLO-QCD}$ and determine the 95% CL exclusion contours at 1/3, 1, and 3 times $\sigma^\text{NLO-QCD}$, to establish how the limit changes with the cross section. This reference cross section $\sigma^\text{NLO-QCD}$ corresponds to gluino pair-production in the limit of infinitely heavy squarks, calculated at NLO using PROSPINO [48] and the CTEQ6 [40] PDFs.

Table 5: Summary of results for the E_T^miss template analysis in the exclusive regions $100\,\text{GeV} < E_\text{T}^\text{miss} < 200\,\text{GeV}$, $200\,\text{GeV} < E_\text{T}^\text{miss} < 300\,\text{GeV}$, and $E_\text{T}^\text{miss} > 300\,\text{GeV}$ for $N_\text{jets} \geq 2$ used for the SMS exclusions of Section 7. The total predicted background (total bkg) is the sum of the Z + jets background predicted from the γ + jets E_T^miss templates method (Z bkg), the background predicted from opposite-flavor events (OF bkg), and the WZ + ZZ background predicted from simulation (VZ bkg). The uncertainties include both the statistical and systematic contributions. For the observed yield (data), the first (second) number in parentheses is the yield in the ee ($\mu\mu$) final state.

	$100\,\text{GeV} < E_\text{T}^\text{miss} < 200\,\text{GeV}$	$200\,\text{GeV} < E_\text{T}^\text{miss} < 300\,\text{GeV}$	$E_\text{T}^\text{miss} > 300\,\text{GeV}$
Z bkg	$33 \pm 4.5 \pm 11$	$1.9 \pm 0.5 \pm 0.6$	$0.4 \pm 0.2 \pm 0.1$
OF bkg	$215 \pm 5.8 \pm 19$	$10 \pm 1.2 \pm 2.7$	$1.6 \pm 0.5 \pm 0.4$
VZ bkg	$29 \pm 0.2 \pm 15$	$4.2 \pm 0.1 \pm 2.1$	$1.2 \pm 0.4 \pm 0.6$
Total bkg	$278 \pm 7.4 \pm 27$	$16 \pm 1.3 \pm 3.5$	$3.2 \pm 0.7 \pm 0.7$
Data	276 (134,142)	14 (8,6)	0

Figure 5 shows the signal selection efficiency times acceptance for the JZB $> 150\,\text{GeV}$ signal region for the topology described above, normalized to the number of events with at least one

leptonically-decaying Z. The 95% CL upper limits on the total gluino pair-production cross section are also shown. The JZB $>$ 250 GeV region has the best sensitivity throughout most of the parameter space of this model. The signal contribution to the Z + jets control sample has been taken into account in these limits. In this mass spectrum, the Z boson and $E_{\mathrm{T}}^{\mathrm{miss}}$ directions are weakly correlated and the sensitivity of the JZB search is reduced at low LSP masses.

Figure 6 shows the signal selection efficiency times acceptance for the $E_{\mathrm{T}}^{\mathrm{miss}} > 100$ GeV signal region in the $E_{\mathrm{T}}^{\mathrm{miss}}$ template analysis, normalized to the number of events with at least one leptonically-decaying Z. The 95% CL upper limits on the total gluino pair-production cross section, based on the three simultaneous counting experiments in the regions 100 GeV $< E_{\mathrm{T}}^{\mathrm{miss}} <$ 200 GeV, 200 $< E_{\mathrm{T}}^{\mathrm{miss}} <$ 300 GeV, and $E_{\mathrm{T}}^{\mathrm{miss}} >$ 300 GeV, are also shown. The signal contribution to the QCD and γ + jets control samples used to estimate the Z background and to the eμ control sample used to estimate the flavor-symmetric background is negligible. This interpretation is based on the results with $N_{\mathrm{jets}} \geq 2$; we find comparable results using $N_{\mathrm{jets}} \geq 3$.

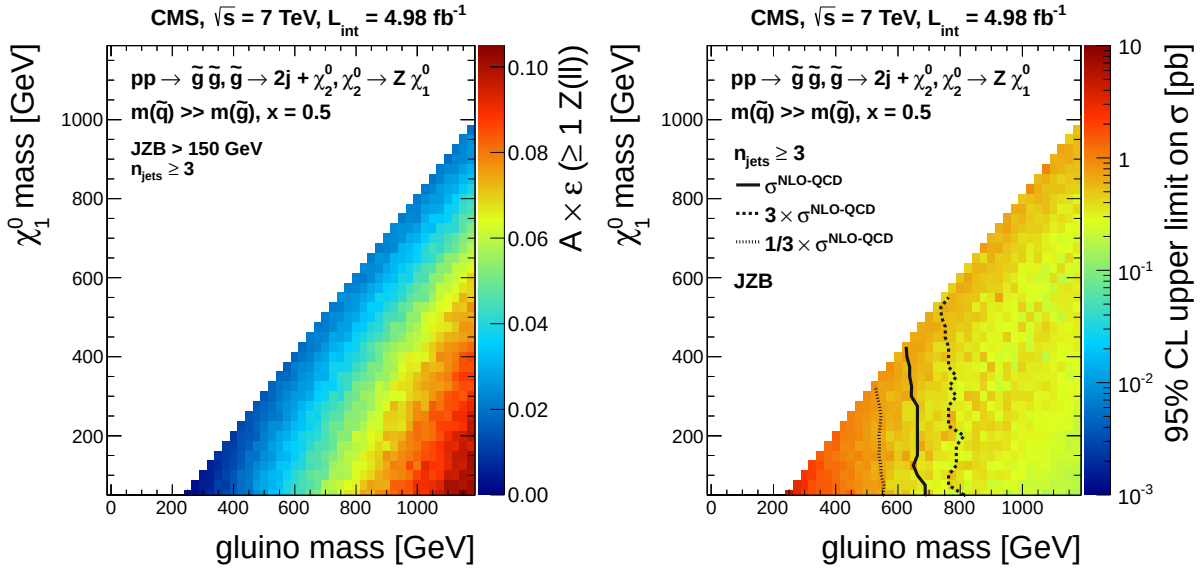

Figure 5: Limits on the SMS topology described in the text, based on the JZB method: (left) signal efficiency times acceptance normalized to the number of events with at least one Z $\to \ell\ell$ decay for the JZB $>$ 150 GeV region; (right) 95% CL upper limits on the total gluino pair-production cross section. The region to the left of the solid contour is excluded assuming that the gluino pair-production cross section is $\sigma^{\mathrm{NLO\text{-}QCD}}$, and that the branching fraction to this SMS topology is 100%. The dotted and dashed contours indicate the excluded region when the cross section is varied by a factor of three. The signal contribution to the control regions is taken into account.

8 Additional Information for Model Testing

Other models of BSM physics in the dilepton final state can be constrained in an approximate manner by simple generator-level studies that compare the expected number of events in 4.98 fb^{-1} with the upper limits from Sections 4.3 and 5.2. The key ingredients of such studies are the kinematic requirements described in this paper, the lepton efficiencies, and the detector responses for $E_{\mathrm{T}}^{\mathrm{miss}}$ and JZB. The trigger efficiencies for events containing ee, eμ, or $\mu\mu$ lepton pairs are 100%, 95%, and 90%, respectively. The muon identification efficiency is approximately 91%; the electron identification efficiency varies approximately linearly from about 83% at $p_{\mathrm{T}} = 20$ GeV to about 93% for $p_{\mathrm{T}} > 60$ GeV and then is flat. The lepton isolation efficiency depends on the lepton momentum, as well as on the jet activity in the event. In $\mathrm{t\bar{t}}$ events, the efficiency varies approximately linearly from about 85% (muons) and 88% (electrons) at

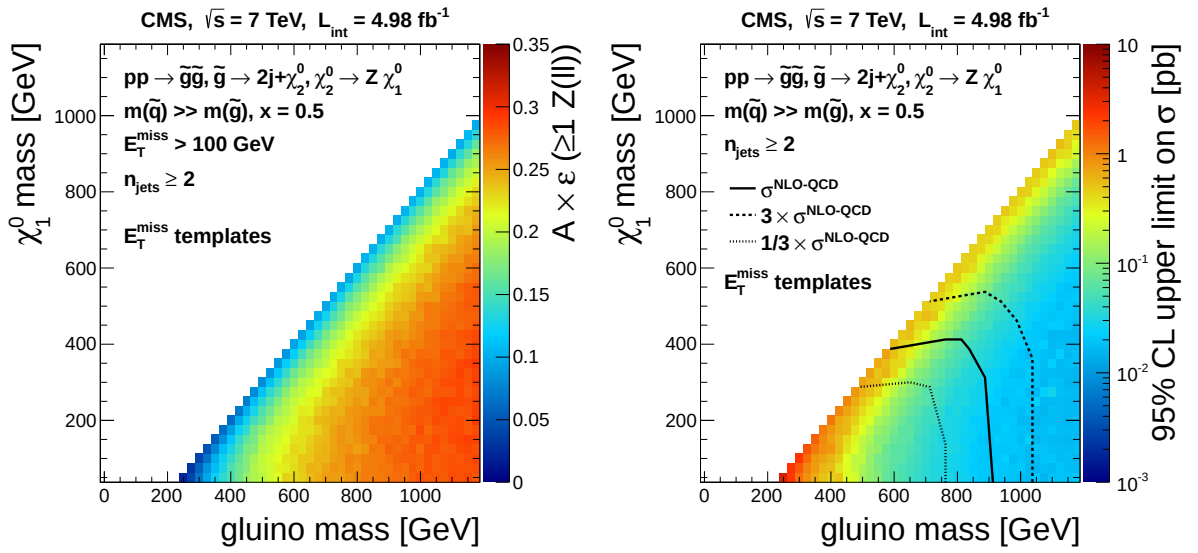

Figure 6: Limits on the SMS topology described in the text, based on the $E_{\mathrm{T}}^{\mathrm{miss}}$ template method: (left) signal efficiency times acceptance normalized to the number of events with at least one $\mathrm{Z} \to \ell\ell$ decay for the $E_{\mathrm{T}}^{\mathrm{miss}} > 100\,\mathrm{GeV}$ region; (right) 95% CL upper limits on the total gluino pair-production cross section. The region to the left of the solid contour is excluded assuming that the gluino pair-production cross section is $\sigma^{\mathrm{NLO\text{-}QCD}}$, and that the branching fraction to this SMS topology is 100%. The dotted and dashed contours indicate the excluded region when the cross section is varied by a factor of three. The signal contribution to the control regions is negligible.

$p_{\mathrm{T}} = 20\,\mathrm{GeV}$ to about 97% for $p_{\mathrm{T}} > 60\,\mathrm{GeV}$. In LM4 (LM8) events, this efficiency is decreased by approximately 5% (10%) over the whole momentum spectrum. The average detector response for JZB is 92%. In order to better quantify the JZB and $E_{\mathrm{T}}^{\mathrm{miss}}$ selection efficiencies, we study the probability for an event to pass a given reconstructed JZB or $E_{\mathrm{T}}^{\mathrm{miss}}$ requirement as a function of the generator-level quantity. Here, generator-level $E_{\mathrm{T}}^{\mathrm{miss}}$ is the negative vector sum of the stable, invisible particles, including neutrinos and SUSY LSP's. The response is parametrized by a function of the form (see Fig. 7):

$$\varepsilon(x) = \varepsilon_{\mathrm{plateau}} \frac{1}{2} \left[\mathrm{erf}\left(\frac{x - x_{\mathrm{thresh}}}{\sigma} \right) + 1 \right]. \tag{2}$$

The fitted parameters are summarised in Table 6.

To approximate the requirement on the jet multiplicity, we count quarks or gluons from the hard scattering process that satisfy the acceptance requirements $p_{\mathrm{T}} > 30\,\mathrm{GeV}$ and $|\eta| < 3.0$. We have tested this efficiency model with the LM4 and LM8 benchmark models, and find that the efficiency from our model is consistent with the expectation from the full reconstruction to within about 15%.

9 Summary

We have performed a search for BSM physics in final states with a leptonically-decaying Z boson, jets, and missing transverse energy. Two complementary strategies are used to suppress the dominant $\mathrm{Z}+\mathrm{jets}$ background and to estimate the remaining background from data control samples: the jet-Z balance method and the $E_{\mathrm{T}}^{\mathrm{miss}}$ template method. Backgrounds from $\mathrm{t\bar{t}}$ processes are estimated using opposite-flavor lepton pairs and dilepton invariant mass sidebands. We find no evidence for anomalous yields beyond standard model (SM) expectations

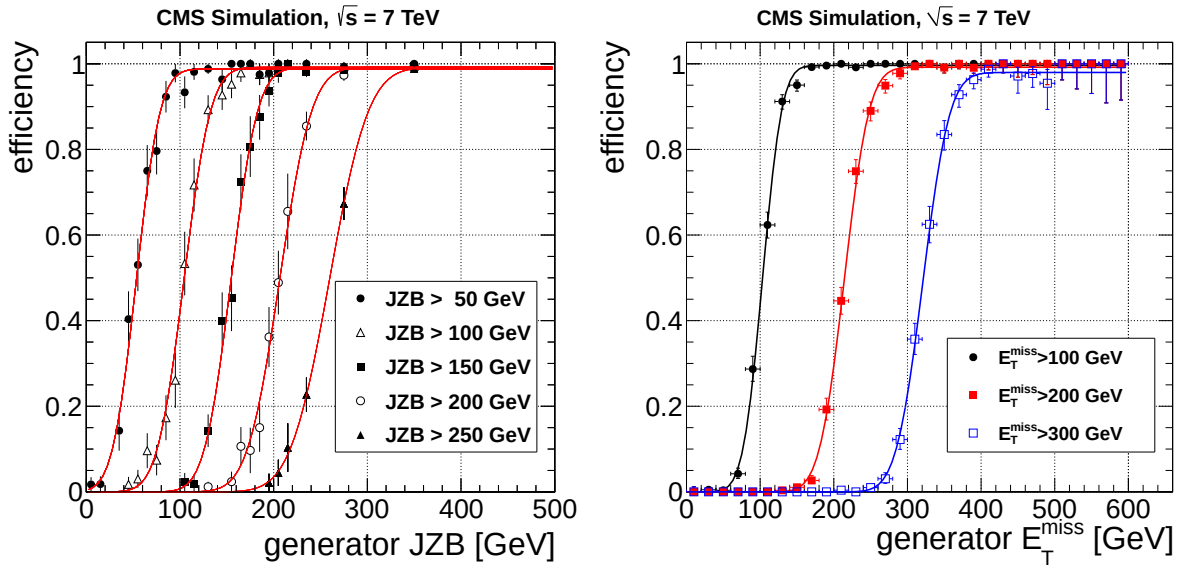

Figure 7: Reconstructed JZB (left) and $E_{\mathrm{T}}^{\mathrm{miss}}$ (right) selection efficiencies as a function of the generator-level quantity, for the different signal regions in the LM4 simulation.

Table 6: Parameters of the JZB (top) and $E_{\mathrm{T}}^{\mathrm{miss}}$ (bottom) response function. The parameter σ is the resolution, x_{thresh} is the JZB or $E_{\mathrm{T}}^{\mathrm{miss}}$ value at the center of the efficiency curve, and $\varepsilon_{\mathrm{plateau}}$ is the efficiency on the plateau.

Region	σ [GeV]	x_{thresh} [GeV]	$\varepsilon_{\mathrm{plateau}}$
JZB $>$ 50 GeV	30	55	0.99
JZB $>$ 100 GeV	30	108	0.99
JZB $>$ 150 GeV	32	156	0.99
JZB $>$ 200 GeV	39	209	0.99
JZB $>$ 250 GeV	45	261	0.98
$E_{\mathrm{T}}^{\mathrm{miss}} > 100$ GeV	29	103	1.00
$E_{\mathrm{T}}^{\mathrm{miss}} > 200$ GeV	38	214	0.99
$E_{\mathrm{T}}^{\mathrm{miss}} > 300$ GeV	40	321	0.98

and place upper limits on the non-SM contributions to the yields in the signal regions. The results are interpreted in the context of simplified model spectra. We also provide information on the detector response and efficiencies to allow tests of BSM models with Z bosons that are not considered in the present study.

Acknowledgments

We wish to congratulate our colleagues in the CERN accelerator departments for the excellent performance of the LHC machine. We thank the technical and administrative staff at CERN and other CMS institutes, and acknowledge support from: FMSR (Austria); FNRS and FWO (Belgium); CNPq, CAPES, FAPERJ, and FAPESP (Brazil); MES (Bulgaria); CERN; CAS, MoST, and NSFC (China); COLCIENCIAS (Colombia); MSES (Croatia); RPF (Cyprus); MoER, SF0690030s09 and ERDF (Estonia); Academy of Finland, MEC, and HIP (Finland); CEA and CNRS/IN2P3 (France); BMBF, DFG, and HGF (Germany); GSRT (Greece); OTKA and NKTH (Hungary); DAE and DST (India); IPM (Iran); SFI (Ireland); INFN (Italy); NRF and WCU (Korea); LAS (Lithuania); CINVESTAV, CONACYT, SEP, and UASLP-FAI (Mexico); MSI (New Zealand); PAEC (Pakistan); MSHE and NSC (Poland); FCT (Portugal); JINR (Armenia, Belarus, Georgia, Ukraine, Uzbekistan); MON, RosAtom, RAS and RFBR (Russia); MSTD (Serbia); MICINN and CPAN (Spain); Swiss Funding Agencies (Switzerland); NSC (Taipei); TUBITAK and TAEK (Turkey); STFC (United Kingdom); DOE and NSF (USA). Individuals have received support from the Marie-Curie programme and the European Research Council (European Union); the Leventis Foundation; the A. P. Sloan Foundation; the Alexander von Humboldt Foundation; the Belgian Federal Science Policy Office; the Fonds pour la Formation à la Recherche dans l'Industrie et dans l'Agriculture (FRIA-Belgium); the Agentschap voor Innovatie door Wetenschap en Technologie (IWT-Belgium); the Council of Science and Industrial Research, India; and the HOMING PLUS programme of Foundation for Polish Science, cofinanced from European Union, Regional Development Fund.

References

[1] CMS Collaboration, "Inclusive search for squarks and gluinos in pp collisions at $\sqrt{s} = 7$ TeV", *Phys. Rev. D* **85** (2012) 012004, doi:10.1103/PhysRevD.85.012004, arXiv:1107.1279.

[2] CMS Collaboration, "Search for supersymmetry in events with b jets and missing transverse momentum at the LHC", *JHEP* **07** (2011) 113, doi:10.1007/JHEP07(2011)113, arXiv:1106.3272.

[3] CMS Collaboration, "Search for Supersymmetry at the LHC in Events with Jets and Missing Transverse Energy", *Phys. Rev. Lett.* **107** (2011) 221804, doi:10.1103/PhysRevLett.107.221804, arXiv:1109.2352.

[4] CMS Collaboration, "Search for supersymmetry in pp collisions at $\sqrt{s} = 7$ TeV in events with a single lepton, jets, and missing transverse momentum", *JHEP* **08** (2011) 156, doi:10.1007/JHEP08(2011)156, arXiv:1107.1870.

[5] CMS Collaboration, "Search for physics beyond the standard model in opposite-sign dilepton events at $\sqrt{s} = 7$TeV", *JHEP* **06** (2011) 026, doi:10.1007/JHEP06(2011)026, arXiv:1103.1348.

[6] CMS Collaboration, "Search for new physics with same-sign isolated dilepton events with jets and missing transverse energy at the LHC", *JHEP* **06** (2011) 077, doi:10.1007/JHEP06(2011)077, arXiv:1104.3168.

[7] CMS Collaboration, "Search for Supersymmetry in pp Collisions at $\sqrt{s} = 7$ TeV in Events with Two Photons and Missing Transverse Energy", *Phys. Rev. Lett.* **106** (2011) 211802, doi:10.1103/PhysRevLett.106.211802, arXiv:1103.0953.

[8] CMS Collaboration, "Search for supersymmetry in events with a lepton, a photon, and large missing transverse energy in pp collisions at $\sqrt{s} = 7$ TeV", *JHEP* **06** (2011) 093, doi:10.1007/JHEP06(2011)093, arXiv:1105.3152.

[9] ATLAS Collaboration, "Searches for supersymmetry with the ATLAS detector using final states with two leptons and missing transverse momentum in $\sqrt{s} = 7$ TeV proton-proton collisions", *Phys. Lett. B* **709** (2012) 137, doi:10.1016/j.physletb.2012.01.076.

[10] ATLAS Collaboration, "Search for supersymmetric particles in events with lepton pairs and large missing transverse momentum in $\sqrt{s} = 7$ TeV proton-proton collisions with the ATLAS experiment", *Eur. Phys. J. C* **71** (2011) 1682, doi:10.1140/epjc/s10052-011-1682-6.

[11] ATLAS Collaboration, "Search for scalar top quark pair production in natural gauge mediated supersymmetry models with the ATLAS detector in pp collisions at sqrt(s) = 7 TeV", (2012). arXiv:1204.6736. Submitted to *Phys. Lett. B*.

[12] Y. Golfand and E. Likhtman, "Extension of the Algebra of Poincare Group Generators and Violation of p Invariance", *JETP Lett.* **13** (1971) 323–326.

[13] J. Wess and B. Zumino, "Supergauge Transformations in Four-Dimensions", *Nucl.Phys.* **B70** (1974) 39–50, doi:10.1016/0550-3213(74)90355-1.

[14] H. P. Nilles, "Supersymmetry, Supergravity and Particle Physics", *Phys.Rept.* **110** (1984) 1–162, doi:10.1016/0370-1573(84)90008-5.

[15] H. E. Haber and G. L. Kane, "The Search for Supersymmetry: Probing Physics Beyond the Standard Model", *Phys.Rept.* **117** (1985) 75–263, doi:10.1016/0370-1573(85)90051-1.

[16] H. Baer, X. Tata, and J. Woodside, "Z^0 + Jets + (Missing) p_T Events as a Signal for Supersymmetry at the Tevatron Collider", *Phys. Rev. D* **42** (1990) 1450, doi:10.1103/PhysRevD.42.1450.

[17] K. T. Matchev and S. D. Thomas, "Higgs and Z Boson Signatures of Supersymmetry", *Phys. Rev. D* **62** (2000) 077702, doi:10.1103/PhysRevD.62.077702.

[18] J. T. Ruderman and D. Shih, "General Neutralino NLSPs at the Early LHC", (2011). arXiv:1103.6083.

[19] S. Ambrosanio, G. L. Kane, G. D. Kribs et al., "Search for Supersymmetry with a Light Gravitino at the Fermilab Tevatron and CERN LEP Colliders", *Phys. Rev. D* **54** (1996) 5395, doi:10.1103/PhysRevD.54.5395, arXiv:hep-ph/9605398.

[20] WMAP Collaboration, "Seven-Year Wilkinson Microwave Anisotropy Probe (WMAP) Observations: Cosmological Interpretation", *Astrophys. J. Suppl.* **192** (2011) 18, doi:10.1088/0067-0049/192/2/18.

[21] J. Ellis et al., "Supersymmetric Relics from the Big Bang", *Nucl. Phys. B* **238** (1984) 453, doi:10.1016/0550-3213(84)90461-9.

[22] P. Fayet, "Supergauge invariant extension of the Higgs mechanism and a model for the electron and its neutrino", *Nucl. Phys. B* **90** (1975) 104, doi:10.1016/0550-3213(75)90636-7.

[23] D. Alves et al., "Simplified Models for LHC New Physics Searches", (2011). arXiv:1105.2838.

[24] N. Arkani-Hamed et al., "MARMOSET: The Path from LHC Data to the New Standard Model via On-Shell Effective Theories", (2007). arXiv:hep-ph/0703088.

[25] B. Knuteson and S. Mrenna, "BARD: Interpreting New Frontier Energy Collider Physics", (2006). arXiv:hep-ph/0602101.

[26] CMS Collaboration, "The CMS Experiment at the CERN LHC", *JINST* **03** (2008) S08004, doi:10.1088/1748-0221/3/08/S08004.

[27] CMS Collaboration, "Electron Reconstruction and Identification at $\sqrt{s} = 7$ TeV", CMS Physics Analysis Summary CMS-PAS-EGM-10-004, (2010).

[28] CMS Collaboration, "Performance of muon identification in pp collisions at $\sqrt{s} = 7$ TeV", CMS Physics Analysis Summary CMS-PAS-MUO-10-002, (2010).

[29] CMS Collaboration, "First Measurement of the Cross Section for Top-Quark Pair Production in Proton-Proton Collisions at $\sqrt{s} = 7$ TeV", *Phys. Lett. B* **695** (2011) 424, doi:10.1016/j.physletb.2010.11.058.

[30] CMS Collaboration, "Determination of jet energy calibration and transverse momentum resolution in CMS", *JINST* **6** (2011) P11002, doi:10.1088/1748-0221/6/11/P11002.

[31] CMS Collaboration, "Commissioning of the Particle-Flow Reconstruction in Minimum-Bias and Jet Events from pp Collisions at 7 TeV", CMS Physics Analysis Summary CMS-PAS-PFT-10-002, (2010).

[32] M. Cacciari, G. P. Salam, and G. Soyez, "The anti-k_t jet clustering algorithm", *JHEP* **04** (2008) 063, doi:10.1088/1126-6708/2008/04/063.

[33] M. Cacciari and G. P. Salam, "Dispelling the N^3 myth for the k_t jet-finder", *Phys. Lett. B* **641** (2006) 57, doi:10.1016/j.physletb.2006.08.037.

[34] M. Cacciari, G. Salam, and G. Soyez, "FastJet user manual", 2011, arXiv:1111.6097.

[35] M. Cacciari and G. P. Salam, "Pileup subtraction using jet areas", *Phys. Lett. B* **659** (2008) 119, doi:10.1016/j.physletb.2007.09.077.

[36] J. Alwall et al., "MadGraph/MadEvent v4: the new web generation", *JHEP* **09** (2007) 028, doi:10.1088/1126-6708/2007/09/028.

[37] T. Sjöstrand, S. Mrenna, and P. Z. Skands, "PYTHIA 6.4 physics and manual", *JHEP* **05** (2006) 026, doi:10.1088/1126-6708/2006/05/026.

[38] G. Kane, "Study of Constrained Minimal Supersymmetry", *Phys. Rev. D* **49** (1994) 6173, doi:10.1103/PhysRevD.49.6173.

[39] CMS Collaboration, "CMS Technical Design Report, Volume II: Physics Performance", *J. Phys. G* **34** (2007) 995, doi:10.1088/0954-3899/34/6/S01.

[40] J. Pumplin et al., "New Generation of Parton Distributions with Uncertainties from Global QCD Analysis", *JHEP* **07** (2002) 012, doi:10.1088/1126-6708/2002/07/012.

[41] S. Agostinelli et al., "GEANT4 – a simulation toolkit", *Nucl. Instr. Meth. A* **506** (2003) 250, doi:10.1016/S0168-9002(03)01368-8.

[42] C. F. Berger et al., "Next-to-Leading Order QCD Predictions for W+3-Jet Distributions at Hadron Colliders", *Phys. Rev. D* **80** (2009) 074036, doi:10.1103/PhysRevD.80.074036.

[43] T. Junk, "Confidence Level Computation for Combining Searches with Small Statistics", *Nucl. Instr. Meth. A* **434** (1999) 435, doi:10.1016/S0168-9002(99)00498-2.

[44] A. L. Read, "Modified Frequentist Analysis of Search Results (the CL_s Method)", in *Workshop on Confidence Limits, Jan 17-18, 2000*, F. James, L. Lyons, and Y. Perrin, eds., p. 81. CERN, Switzerland, 2000.

[45] V. Pavlunin, "Modeling Missing Transverse Energy in V+jets at CERN LHC", *Phys. Rev. D* **81** (2010) 035005, doi:10.1103/PhysRevD.81.035005.

[46] D. Bourilkov, R. C. Group, and M. R. Whalley, "LHAPDF: PDF Use from the Tevatron to the LHC", (2006). arXiv:hep-ph/0605240.

[47] CMS Collaboration, "Absolute Calibration of the Luminosity Measurement at CMS: Winter 2012 Update", CMS Physics Analysis Summary CMS-PAS-SMP-12-008, (2012).

[48] W. Beenakker, R. Hopker, and M. Spira, "PROSPINO: A Program for the Production of Supersymmetric Particles in Next-to-Leading Order QCD", (1996). arXiv:hep-ph/9611232.

A Additional Interpretation of the Results

In this appendix we interpret our results in the context of two additional SMS topologies. The first topology is the same as discussed in Sec. 7, in which the LSP is the lightest neutralino, but with a different choice of the $\widetilde{\chi}_2^0$ mass parameter, $x = 0.75$, so that the $\widetilde{\chi}_2^0$ is closer in mass to the gluino than to the LSP. The second is a topology inspired by gauge-mediated SUSY-breaking (GMSB) models, in which the LSP is a light gravitino (mass $\lesssim 1$ keV), which is treated here as massless. In this scenario, we consider gluino pair-production where each gluino decays to a pair of jets and the lightest neutralino $\widetilde{\chi}_1^0$, which itself decays to a Z boson and the gravitino ($\tilde{G}$) LSP, as shown in Fig. 8. If the $\widetilde{\chi}_1^0$ is mostly bino then the decay $\widetilde{\chi}_1^0 \to \gamma\, \tilde{G}$ dominates, while the decay $\widetilde{\chi}_1^0 \to \mathrm{Z}\, \tilde{G}$ can become favored if the $\widetilde{\chi}_1^0$ is mostly wino or higgsino. The parameters of this model are the masses of the gluino and of the lightest neutralino $\widetilde{\chi}_1^0$.

Results for the neutralino LSP scenario are presented in Fig. 9 (JZB analysis) and Fig. 10 (MET analysis). Results for the gravitino LSP scenario are presented in Fig. 11 (JZB analysis) and Fig. 12 (MET analysis).

The JZB search relies on the correlation between the Z boson and the $E_{\mathrm{T}}^{\mathrm{miss}}$ directions, which leads to an asymmetry in the JZB distribution. The sensitivity of this search is thus reduced in mass spectra that lead to symmetric JZB, as can be the case in the GMSB-inspired scenario in the region of parameter space that is evident, e.g., in Fig. 11.

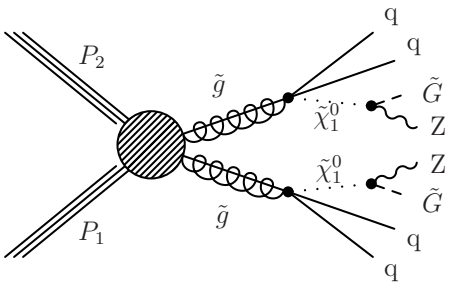

Figure 8: Simplified model for the production of two gluinos decaying into two Z bosons, two gravitinos, and jets.

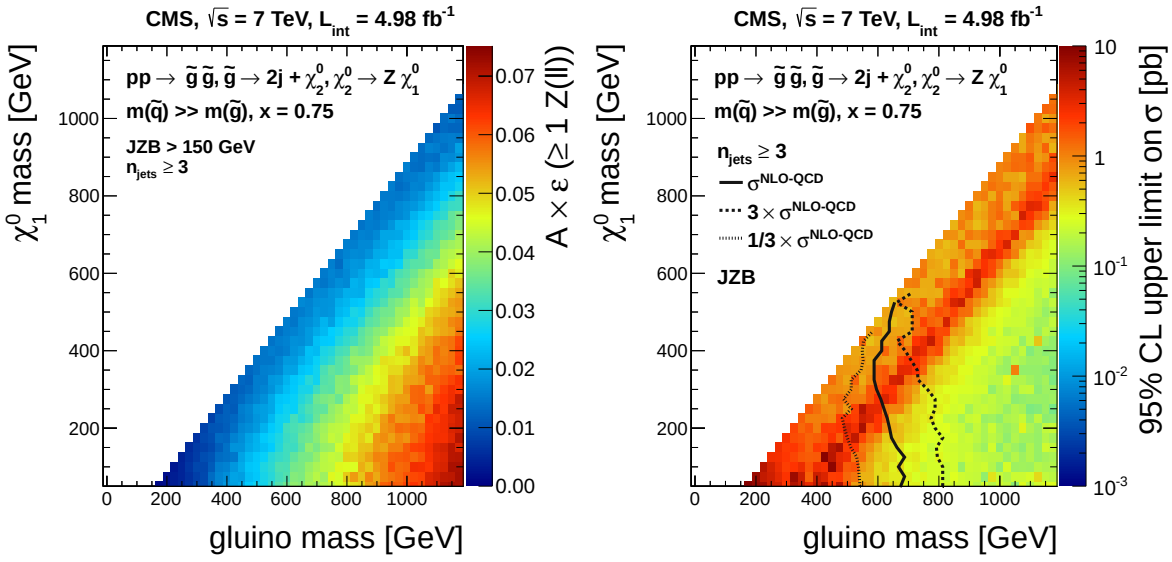

Figure 9: Limits on the SMS topology with neutralino LSP ($x = 0.75$), based on the JZB method: (left) signal efficiency times acceptance normalized to the number of events with at least one $Z \to \ell\ell$ decay for the JZB $>$ 150 GeV region; (right) 95% CL upper limits on the total gluino pair-production cross section. The region to the left of the solid contour is excluded assuming that the gluino pair-production cross section is $\sigma^{\text{NLO-QCD}}$, and that the branching fraction to this SMS topology is 100%. The dotted and dashed contours indicate the excluded region when the cross section is varied by a factor of three. The signal contribution to the control regions is taken into account.

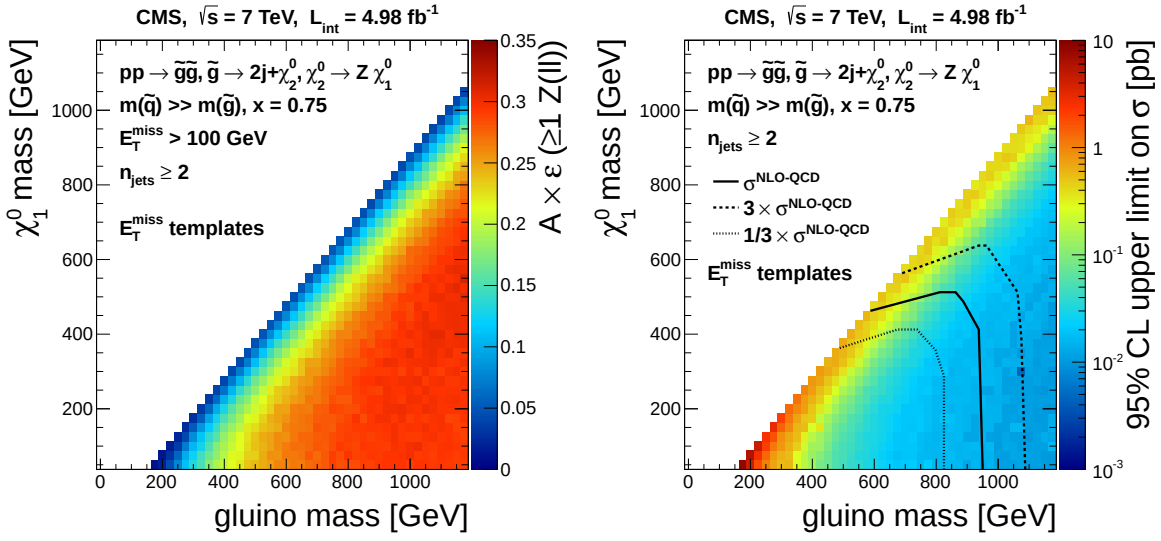

Figure 10: Limits on the SMS topology with neutralino LSP ($x = 0.75$), based on the $E_{\text{T}}^{\text{miss}}$ template method: (left) signal efficiency times acceptance normalized to the number of events with at least one $Z \to \ell\ell$ decay for the $E_{\text{T}}^{\text{miss}} > 100$ GeV region; (right) 95% CL upper limits on the total gluino pair-production cross section. The region to the left of the solid contour is excluded assuming that the gluino pair-production cross section is $\sigma^{\text{NLO-QCD}}$, and that the branching fraction to this SMS topology is 100%. The dotted and dashed contours indicate the excluded region when the cross section is varied by a factor of three. The signal contribution to the control regions is negligible.

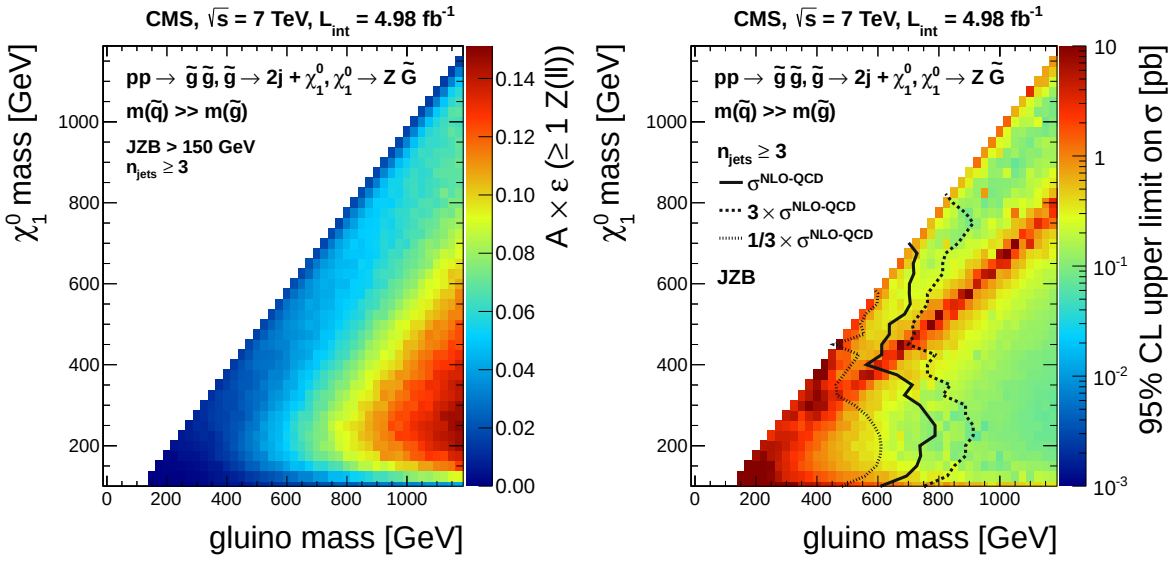

Figure 11: Limits on the SMS topology with gravitino LSP, based on the JZB method: (left) signal efficiency times acceptance normalized to the number of events with at least one $Z \to \ell\ell$ decay for the JZB > 150 GeV region; (right) 95% CL upper limits on the total gluino pair-production cross section. The region to the left of the solid contour is excluded assuming that the gluino pair-production cross section is $\sigma^{\text{NLO-QCD}}$, and that the branching fraction to this SMS topology is 100%. The dotted and dashed contours indicate the excluded region when the cross section is varied by a factor of three. The signal contribution to the control regions is taken into account.

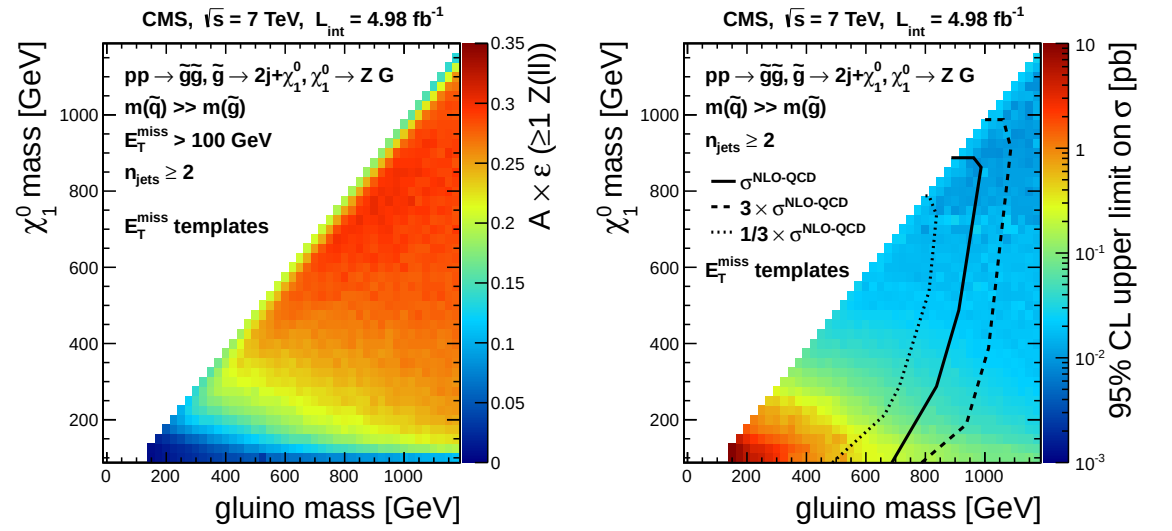

Figure 12: Limits on the SMS topology with gravitino LSP, based on the $E_{\mathrm{T}}^{\mathrm{miss}}$ template method: (left) signal efficiency times acceptance normalized to the number of events with at least one $Z \to \ell\ell$ decay for the $E_{\mathrm{T}}^{\mathrm{miss}} > 100$ GeV region; (right) 95% CL upper limits on the total gluino pair-production cross section. The region to the left of the solid contour is excluded assuming that the gluino pair-production cross section is $\sigma^{\text{NLO-QCD}}$, and that the branching fraction to this SMS topology is 100%. The dotted and dashed contours indicate the excluded region when the cross section is varied by a factor of three. The signal contribution to the control regions is negligible.

B The CMS Collaboration

Yerevan Physics Institute, Yerevan, Armenia
S. Chatrchyan, V. Khachatryan, A.M. Sirunyan, A. Tumasyan

Institut für Hochenergiephysik der OeAW, Wien, Austria
W. Adam, T. Bergauer, M. Dragicevic, J. Erö, C. Fabjan, M. Friedl, R. Frühwirth, V.M. Ghete, J. Hammer[1], N. Hörmann, J. Hrubec, M. Jeitler, W. Kiesenhofer, M. Krammer, D. Liko, I. Mikulec, M. Pernicka[†], B. Rahbaran, C. Rohringer, H. Rohringer, R. Schöfbeck, J. Strauss, A. Taurok, F. Teischinger, P. Wagner, W. Waltenberger, G. Walzel, E. Widl, C.-E. Wulz

National Centre for Particle and High Energy Physics, Minsk, Belarus
V. Mossolov, N. Shumeiko, J. Suarez Gonzalez

Universiteit Antwerpen, Antwerpen, Belgium
S. Bansal, K. Cerny, T. Cornelis, E.A. De Wolf, X. Janssen, S. Luyckx, T. Maes, L. Mucibello, S. Ochesanu, B. Roland, R. Rougny, M. Selvaggi, H. Van Haevermaet, P. Van Mechelen, N. Van Remortel, A. Van Spilbeeck

Vrije Universiteit Brussel, Brussel, Belgium
F. Blekman, S. Blyweert, J. D'Hondt, R. Gonzalez Suarez, A. Kalogeropoulos, M. Maes, A. Olbrechts, W. Van Doninck, P. Van Mulders, G.P. Van Onsem, I. Villella

Université Libre de Bruxelles, Bruxelles, Belgium
O. Charaf, B. Clerbaux, G. De Lentdecker, V. Dero, A.P.R. Gay, T. Hreus, A. Léonard, P.E. Marage, L. Thomas, C. Vander Velde, P. Vanlaer

Ghent University, Ghent, Belgium
V. Adler, K. Beernaert, A. Cimmino, S. Costantini, G. Garcia, M. Grunewald, B. Klein, J. Lellouch, A. Marinov, J. Mccartin, A.A. Ocampo Rios, D. Ryckbosch, N. Strobbe, F. Thyssen, M. Tytgat, L. Vanelderen, P. Verwilligen, S. Walsh, E. Yazgan, N. Zaganidis

Université Catholique de Louvain, Louvain-la-Neuve, Belgium
S. Basegmez, G. Bruno, L. Ceard, C. Delaere, T. du Pree, D. Favart, L. Forthomme, A. Giammanco[2], J. Hollar, V. Lemaitre, J. Liao, O. Militaru, C. Nuttens, D. Pagano, A. Pin, K. Piotrzkowski, N. Schul

Université de Mons, Mons, Belgium
N. Beliy, T. Caebergs, E. Daubie, G.H. Hammad

Centro Brasileiro de Pesquisas Fisicas, Rio de Janeiro, Brazil
G.A. Alves, M. Correa Martins Junior, D. De Jesus Damiao, T. Martins, M.E. Pol, M.H.G. Souza

Universidade do Estado do Rio de Janeiro, Rio de Janeiro, Brazil
W.L. Aldá Júnior, W. Carvalho, A. Custódio, E.M. Da Costa, C. De Oliveira Martins, S. Fonseca De Souza, D. Matos Figueiredo, L. Mundim, H. Nogima, V. Oguri, W.L. Prado Da Silva, A. Santoro, S.M. Silva Do Amaral, L. Soares Jorge, A. Sznajder

Instituto de Fisica Teorica, Universidade Estadual Paulista, Sao Paulo, Brazil
T.S. Anjos[3], C.A. Bernardes[3], F.A. Dias[4], T.R. Fernandez Perez Tomei, E. M. Gregores[3], C. Lagana, F. Marinho, P.G. Mercadante[3], S.F. Novaes, Sandra S. Padula

Institute for Nuclear Research and Nuclear Energy, Sofia, Bulgaria
V. Genchev[1], P. Iaydjiev[1], S. Piperov, M. Rodozov, S. Stoykova, G. Sultanov, V. Tcholakov, R. Trayanov, M. Vutova

University of Sofia, Sofia, Bulgaria
A. Dimitrov, R. Hadjiiska, A. Karadzhinova, V. Kozhuharov, L. Litov, B. Pavlov, P. Petkov

Institute of High Energy Physics, Beijing, China
J.G. Bian, G.M. Chen, H.S. Chen, C.H. Jiang, D. Liang, S. Liang, X. Meng, J. Tao, J. Wang, J. Wang, X. Wang, Z. Wang, H. Xiao, M. Xu, J. Zang, Z. Zhang

State Key Lab. of Nucl. Phys. and Tech., Peking University, Beijing, China
C. Asawatangtrakuldee, Y. Ban, S. Guo, Y. Guo, W. Li, S. Liu, Y. Mao, S.J. Qian, H. Teng, S. Wang, B. Zhu, W. Zou

Universidad de Los Andes, Bogota, Colombia
C. Avila, B. Gomez Moreno, A.F. Osorio Oliveros, J.C. Sanabria

Technical University of Split, Split, Croatia
N. Godinovic, D. Lelas, R. Plestina[5], D. Polic, I. Puljak[1]

University of Split, Split, Croatia
Z. Antunovic, M. Dzelalija, M. Kovac

Institute Rudjer Boskovic, Zagreb, Croatia
V. Brigljevic, S. Duric, K. Kadija, J. Luetic, S. Morovic

University of Cyprus, Nicosia, Cyprus
A. Attikis, M. Galanti, G. Mavromanolakis, J. Mousa, C. Nicolaou, F. Ptochos, P.A. Razis

Charles University, Prague, Czech Republic
M. Finger, M. Finger Jr.

Academy of Scientific Research and Technology of the Arab Republic of Egypt, Egyptian Network of High Energy Physics, Cairo, Egypt
Y. Assran[6], S. Elgammal[7], A. Ellithi Kamel[8], S. Khalil[9], M.A. Mahmoud[10], A. Radi[9,11]

National Institute of Chemical Physics and Biophysics, Tallinn, Estonia
M. Kadastik, M. Müntel, M. Raidal, L. Rebane, A. Tiko

Department of Physics, University of Helsinki, Helsinki, Finland
V. Azzolini, P. Eerola, G. Fedi, M. Voutilainen

Helsinki Institute of Physics, Helsinki, Finland
S. Czellar, J. Härkönen, A. Heikkinen, V. Karimäki, R. Kinnunen, M.J. Kortelainen, T. Lampén, K. Lassila-Perini, S. Lehti, T. Lindén, P. Luukka, T. Mäenpää, T. Peltola, E. Tuominen, J. Tuominiemi, E. Tuovinen, D. Ungaro, L. Wendland

Lappeenranta University of Technology, Lappeenranta, Finland
K. Banzuzi, A. Korpela, T. Tuuva

Laboratoire d'Annecy-le-Vieux de Physique des Particules, IN2P3-CNRS, Annecy-le-Vieux, France
D. Sillou

DSM/IRFU, CEA/Saclay, Gif-sur-Yvette, France
M. Besancon, S. Choudhury, M. Dejardin, D. Denegri, B. Fabbro, J.L. Faure, F. Ferri, S. Ganjour, A. Givernaud, P. Gras, G. Hamel de Monchenault, P. Jarry, E. Locci, J. Malcles, L. Millischer, J. Rander, A. Rosowsky, I. Shreyber, M. Titov

Laboratoire Leprince-Ringuet, Ecole Polytechnique, IN2P3-CNRS, Palaiseau, France
S. Baffioni, F. Beaudette, L. Benhabib, L. Bianchini, M. Bluj[12], C. Broutin, P. Busson, C. Charlot, N. Daci, T. Dahms, L. Dobrzynski, R. Granier de Cassagnac, M. Haguenauer, P. Miné, C. Mironov, C. Ochando, P. Paganini, D. Sabes, R. Salerno, Y. Sirois, C. Veelken, A. Zabi

Institut Pluridisciplinaire Hubert Curien, Université de Strasbourg, Université de Haute Alsace Mulhouse, CNRS/IN2P3, Strasbourg, France
J.-L. Agram[13], J. Andrea, D. Bloch, D. Bodin, J.-M. Brom, M. Cardaci, E.C. Chabert, C. Collard, E. Conte[13], F. Drouhin[13], C. Ferro, J.-C. Fontaine[13], D. Gelé, U. Goerlach, P. Juillot, M. Karim[13], A.-C. Le Bihan, P. Van Hove

Centre de Calcul de l'Institut National de Physique Nucleaire et de Physique des Particules (IN2P3), Villeurbanne, France
F. Fassi, D. Mercier

Université de Lyon, Université Claude Bernard Lyon 1, CNRS-IN2P3, Institut de Physique Nucléaire de Lyon, Villeurbanne, France
C. Baty, S. Beauceron, N. Beaupere, M. Bedjidian, O. Bondu, G. Boudoul, D. Boumediene, H. Brun, J. Chasserat, R. Chierici[1], D. Contardo, P. Depasse, H. El Mamouni, A. Falkiewicz, J. Fay, S. Gascon, M. Gouzevitch, B. Ille, T. Kurca, T. Le Grand, M. Lethuillier, L. Mirabito, S. Perries, V. Sordini, S. Tosi, Y. Tschudi, P. Verdier, S. Viret

E. Andronikashvili Institute of Physics, Academy of Science, Tbilisi, Georgia
L. Rurua

RWTH Aachen University, I. Physikalisches Institut, Aachen, Germany
G. Anagnostou, S. Beranek, M. Edelhoff, L. Feld, N. Heracleous, O. Hindrichs, R. Jussen, K. Klein, J. Merz, A. Ostapchuk, A. Perieanu, F. Raupach, J. Sammet, S. Schael, D. Sprenger, H. Weber, B. Wittmer, V. Zhukov[14]

RWTH Aachen University, III. Physikalisches Institut A, Aachen, Germany
M. Ata, J. Caudron, E. Dietz-Laursonn, M. Erdmann, A. Güth, T. Hebbeker, C. Heidemann, K. Hoepfner, T. Klimkovich, D. Klingebiel, P. Kreuzer, D. Lanske†, J. Lingemann, C. Magass, M. Merschmeyer, A. Meyer, M. Olschewski, P. Papacz, H. Pieta, H. Reithler, S.A. Schmitz, L. Sonnenschein, J. Steggemann, D. Teyssier, M. Weber

RWTH Aachen University, III. Physikalisches Institut B, Aachen, Germany
M. Bontenackels, V. Cherepanov, M. Davids, G. Flügge, H. Geenen, M. Geisler, W. Haj Ahmad, F. Hoehle, B. Kargoll, T. Kress, Y. Kuessel, A. Linn, A. Nowack, L. Perchalla, O. Pooth, J. Rennefeld, P. Sauerland, A. Stahl

Deutsches Elektronen-Synchrotron, Hamburg, Germany
M. Aldaya Martin, J. Behr, W. Behrenhoff, U. Behrens, M. Bergholz[15], A. Bethani, K. Borras, A. Burgmeier, A. Cakir, L. Calligaris, A. Campbell, E. Castro, F. Costanza, D. Dammann, G. Eckerlin, D. Eckstein, G. Flucke, A. Geiser, I. Glushkov, S. Habib, J. Hauk, H. Jung[1], M. Kasemann, P. Katsas, C. Kleinwort, H. Kluge, A. Knutsson, M. Krämer, D. Krücker, E. Kuznetsova, W. Lange, W. Lohmann[15], B. Lutz, R. Mankel, I. Marfin, M. Marienfeld, I.-A. Melzer-Pellmann, A.B. Meyer, J. Mnich, A. Mussgiller, S. Naumann-Emme, J. Olzem, H. Perrey, A. Petrukhin, D. Pitzl, A. Raspereza, P.M. Ribeiro Cipriano, C. Riedl, M. Rosin, J. Salfeld-Nebgen, R. Schmidt[15], T. Schoerner-Sadenius, N. Sen, A. Spiridonov, M. Stein, R. Walsh, C. Wissing

University of Hamburg, Hamburg, Germany
C. Autermann, V. Blobel, S. Bobrovskyi, J. Draeger, H. Enderle, J. Erfle, U. Gebbert, M. Görner,

T. Hermanns, R.S. Höing, K. Kaschube, G. Kaussen, H. Kirschenmann, R. Klanner, J. Lange, B. Mura, F. Nowak, N. Pietsch, D. Rathjens, C. Sander, H. Schettler, P. Schleper, E. Schlieckau, A. Schmidt, M. Schröder, T. Schum, M. Seidel, H. Stadie, G. Steinbrück, J. Thomsen

Institut für Experimentelle Kernphysik, Karlsruhe, Germany
C. Barth, J. Berger, T. Chwalek, W. De Boer, A. Dierlamm, M. Feindt, M. Guthoff[1], C. Hackstein, F. Hartmann, M. Heinrich, H. Held, K.H. Hoffmann, S. Honc, U. Husemann, I. Katkov[14], J.R. Komaragiri, D. Martschei, S. Mueller, Th. Müller, M. Niegel, A. Nürnberg, O. Oberst, A. Oehler, J. Ott, T. Peiffer, G. Quast, K. Rabbertz, F. Ratnikov, N. Ratnikova, S. Röcker, C. Saout, A. Scheurer, F.-P. Schilling, M. Schmanau, G. Schott, H.J. Simonis, F.M. Stober, D. Troendle, R. Ulrich, J. Wagner-Kuhr, T. Weiler, M. Zeise, E.B. Ziebarth

Institute of Nuclear Physics "Demokritos", Aghia Paraskevi, Greece
G. Daskalakis, T. Geralis, S. Kesisoglou, A. Kyriakis, D. Loukas, I. Manolakos, A. Markou, C. Markou, C. Mavrommatis, E. Ntomari

University of Athens, Athens, Greece
L. Gouskos, T.J. Mertzimekis, A. Panagiotou, N. Saoulidou

University of Ioánnina, Ioánnina, Greece
I. Evangelou, C. Foudas[1], P. Kokkas, N. Manthos, I. Papadopoulos, V. Patras

KFKI Research Institute for Particle and Nuclear Physics, Budapest, Hungary
A. Aranyi, G. Bencze, L. Boldizsar, C. Hajdu[1], P. Hidas, D. Horvath[16], A. Kapusi, K. Krajczar[17], B. Radics, F. Sikler[1], V. Veszpremi, G. Vesztergombi[17]

Institute of Nuclear Research ATOMKI, Debrecen, Hungary
N. Beni, J. Molnar, J. Palinkas, Z. Szillasi

University of Debrecen, Debrecen, Hungary
J. Karancsi, P. Raics, Z.L. Trocsanyi, B. Ujvari

Panjab University, Chandigarh, India
S.B. Beri, V. Bhatnagar, N. Dhingra, R. Gupta, M. Jindal, M. Kaur, J.M. Kohli, M.Z. Mehta, N. Nishu, L.K. Saini, A. Sharma, A.P. Singh, J. Singh, S.P. Singh

University of Delhi, Delhi, India
S. Ahuja, B.C. Choudhary, A. Kumar, A. Kumar, S. Malhotra, M. Naimuddin, K. Ranjan, V. Sharma, R.K. Shivpuri

Saha Institute of Nuclear Physics, Kolkata, India
S. Banerjee, S. Bhattacharya, S. Dutta, B. Gomber, Sa. Jain, Sh. Jain, R. Khurana, S. Sarkar

Bhabha Atomic Research Centre, Mumbai, India
A. Abdulsalam, R.K. Choudhury, D. Dutta, S. Kailas, V. Kumar, A.K. Mohanty[1], L.M. Pant, P. Shukla

Tata Institute of Fundamental Research - EHEP, Mumbai, India
T. Aziz, S. Ganguly, M. Guchait[18], A. Gurtu[19], M. Maity[20], G. Majumder, K. Mazumdar, G.B. Mohanty, B. Parida, K. Sudhakar, N. Wickramage

Tata Institute of Fundamental Research - HECR, Mumbai, India
S. Banerjee, S. Dugad

Institute for Research in Fundamental Sciences (IPM), Tehran, Iran
H. Arfaei, H. Bakhshiansohi[21], S.M. Etesami[22], A. Fahim[21], M. Hashemi, H. Hesari, A. Jafari[21],

M. Khakzad, A. Mohammadi[23], M. Mohammadi Najafabadi, S. Paktinat Mehdiabadi, B. Safarzadeh[24], M. Zeinali[22]

INFN Sezione di Bari [a], Università di Bari [b], Politecnico di Bari [c], Bari, Italy
M. Abbrescia[a,b], L. Barbone[a,b], C. Calabria[a,b,1], S.S. Chhibra[a,b], A. Colaleo[a], D. Creanza[a,c], N. De Filippis[a,c,1], M. De Palma[a,b], L. Fiore[a], G. Iaselli[a,c], L. Lusito[a,b], G. Maggi[a,c], M. Maggi[a], B. Marangelli[a,b], S. My[a,c], S. Nuzzo[a,b], N. Pacifico[a,b], A. Pompili[a,b], G. Pugliese[a,c], G. Selvaggi[a,b], L. Silvestris[a], G. Singh[a,b], G. Zito[a]

INFN Sezione di Bologna [a], Università di Bologna [b], Bologna, Italy
G. Abbiendi[a], A.C. Benvenuti[a], D. Bonacorsi[a,b], S. Braibant-Giacomelli[a,b], L. Brigliadori[a,b], P. Capiluppi[a,b], A. Castro[a,b], F.R. Cavallo[a], M. Cuffiani[a,b], G.M. Dallavalle[a], F. Fabbri[a], A. Fanfani[a,b], D. Fasanella[a,b,1], P. Giacomelli[a], C. Grandi[a], L. Guiducci, S. Marcellini[a], G. Masetti[a], M. Meneghelli[a,b,1], A. Montanari[a], F.L. Navarria[a,b], F. Odorici[a], A. Perrotta[a], F. Primavera[a,b], A.M. Rossi[a,b], T. Rovelli[a,b], G. Siroli[a,b], R. Travaglini[a,b]

INFN Sezione di Catania [a], Università di Catania [b], Catania, Italy
S. Albergo[a,b], G. Cappello[a,b], M. Chiorboli[a,b], S. Costa[a,b], R. Potenza[a,b], A. Tricomi[a,b], C. Tuve[a,b]

INFN Sezione di Firenze [a], Università di Firenze [b], Firenze, Italy
G. Barbagli[a], V. Ciulli[a,b], C. Civinini[a], R. D'Alessandro[a,b], E. Focardi[a,b], S. Frosali[a,b], E. Gallo[a], S. Gonzi[a,b], M. Meschini[a], S. Paoletti[a], G. Sguazzoni[a], A. Tropiano[a,1]

INFN Laboratori Nazionali di Frascati, Frascati, Italy
L. Benussi, S. Bianco, S. Colafranceschi[25], F. Fabbri, D. Piccolo

INFN Sezione di Genova, Genova, Italy
P. Fabbricatore, R. Musenich

INFN Sezione di Milano-Bicocca [a], Università di Milano-Bicocca [b], Milano, Italy
A. Benaglia[a,b,1], F. De Guio[a,b], L. Di Matteo[a,b,1], S. Fiorendi[a,b], S. Gennai[a,1], A. Ghezzi[a,b], S. Malvezzi[a], R.A. Manzoni[a,b], A. Martelli[a,b], A. Massironi[a,b,1], D. Menasce[a], L. Moroni[a], M. Paganoni[a,b], D. Pedrini[a], S. Ragazzi[a,b], N. Redaelli[a], S. Sala[a], T. Tabarelli de Fatis[a,b]

INFN Sezione di Napoli [a], Università di Napoli "Federico II" [b], Napoli, Italy
S. Buontempo[a], C.A. Carrillo Montoya[a,1], N. Cavallo[a,26], A. De Cosa[a,b], O. Dogangun[a,b], F. Fabozzi[a,26], A.O.M. Iorio[a,1], L. Lista[a], S. Meola[a,27], M. Merola[a,b], P. Paolucci[a]

INFN Sezione di Padova [a], Università di Padova [b], Università di Trento (Trento) [c], Padova, Italy
P. Azzi[a], N. Bacchetta[a,1], P. Bellan[a,b], D. Bisello[a,b], A. Branca[a,1], R. Carlin[a,b], P. Checchia[a], T. Dorigo[a], F. Gasparini[a,b], A. Gozzelino[a], K. Kanishchev[a,c], S. Lacaprara[a,28], I. Lazzizzera[a,c], M. Margoni[a,b], A.T. Meneguzzo[a,b], M. Nespolo[a,1], L. Perrozzi[a], N. Pozzobon[a,b], P. Ronchese[a,b], F. Simonetto[a,b], E. Torassa[a], M. Tosi[a,b,1], S. Vanini[a,b], P. Zotto[a,b], G. Zumerle[a,b]

INFN Sezione di Pavia [a], Università di Pavia [b], Pavia, Italy
M. Gabusi[a,b], S.P. Ratti[a,b], C. Riccardi[a,b], P. Torre[a,b], P. Vitulo[a,b]

INFN Sezione di Perugia [a], Università di Perugia [b], Perugia, Italy
G.M. Bilei[a], B. Caponeri[a,b], L. Fanò[a,b], P. Lariccia[a,b], A. Lucaroni[a,b,1], G. Mantovani[a,b], M. Menichelli[a], A. Nappi[a,b], F. Romeo[a,b], A. Saha, A. Santocchia[a,b], S. Taroni[a,b,1]

INFN Sezione di Pisa [a], Università di Pisa [b], Scuola Normale Superiore di Pisa [c], Pisa, Italy
P. Azzurri[a,c], G. Bagliesi[a], T. Boccali[a], G. Broccolo[a,c], R. Castaldi[a], R.T. D'Agnolo[a,c], R. Dell'Orso[a], F. Fiori[a,b], L. Foà[a,c], A. Giassi[a], A. Kraan[a], F. Ligabue[a,c], T. Lomtadze[a],

L. Martini[a,29], A. Messineo[a,b], F. Palla[a], F. Palmonari[a], A. Rizzi[a,b], A.T. Serban[a,30], P. Spagnolo[a], R. Tenchini[a], G. Tonelli[a,b,1], A. Venturi[a,1], P.G. Verdini[a]

INFN Sezione di Roma [a], Università di Roma "La Sapienza" [b], Roma, Italy
L. Barone[a,b], F. Cavallari[a], D. Del Re[a,b,1], M. Diemoz[a], C. Fanelli[a,b], M. Grassi[a,1], E. Longo[a,b], P. Meridiani[a,1], F. Micheli[a,b], S. Nourbakhsh[a], G. Organtini[a,b], F. Pandolfi[a,b], R. Paramatti[a], S. Rahatlou[a,b], M. Sigamani[a], L. Soffi[a,b]

INFN Sezione di Torino [a], Università di Torino [b], Università del Piemonte Orientale (Novara) [c], Torino, Italy
N. Amapane[a,b], R. Arcidiacono[a,c], S. Argiro[a,b], M. Arneodo[a,c], C. Biino[a], C. Botta[a,b], N. Cartiglia[a], R. Castello[a,b], M. Costa[a,b], G. Dellacasa[a], N. Demaria[a], A. Graziano[a,b], C. Mariotti[a,1], S. Maselli[a], E. Migliore[a,b], V. Monaco[a,b], M. Musich[a,1], M.M. Obertino[a,c], N. Pastrone[a], M. Pelliccioni[a], A. Potenza[a,b], A. Romero[a,b], M. Ruspa[a,c], R. Sacchi[a,b], A. Solano[a,b], A. Staiano[a], A. Vilela Pereira[a]

INFN Sezione di Trieste [a], Università di Trieste [b], Trieste, Italy
S. Belforte[a], F. Cossutti[a], G. Della Ricca[a,b], B. Gobbo[a], M. Marone[a,b,1], D. Montanino[a,b,1], A. Penzo[a], A. Schizzi[a,b]

Kangwon National University, Chunchon, Korea
S.G. Heo, T.Y. Kim, S.K. Nam

Kyungpook National University, Daegu, Korea
S. Chang, J. Chung, D.H. Kim, G.N. Kim, D.J. Kong, H. Park, S.R. Ro, D.C. Son

Chonnam National University, Institute for Universe and Elementary Particles, Kwangju, Korea
J.Y. Kim, Zero J. Kim, S. Song

Konkuk University, Seoul, Korea
H.Y. Jo

Korea University, Seoul, Korea
S. Choi, D. Gyun, B. Hong, M. Jo, H. Kim, T.J. Kim, K.S. Lee, D.H. Moon, S.K. Park, E. Seo

University of Seoul, Seoul, Korea
M. Choi, S. Kang, H. Kim, J.H. Kim, C. Park, I.C. Park, S. Park, G. Ryu

Sungkyunkwan University, Suwon, Korea
Y. Cho, Y. Choi, Y.K. Choi, J. Goh, M.S. Kim, B. Lee, J. Lee, S. Lee, H. Seo, I. Yu

Vilnius University, Vilnius, Lithuania
M.J. Bilinskas, I. Grigelionis, M. Janulis, A. Juodagalvis

Centro de Investigacion y de Estudios Avanzados del IPN, Mexico City, Mexico
H. Castilla-Valdez, E. De La Cruz-Burelo, I. Heredia-de La Cruz, R. Lopez-Fernandez, R. Magaña Villalba, J. Martínez-Ortega, A. Sánchez-Hernández, L.M. Villasenor-Cendejas

Universidad Iberoamericana, Mexico City, Mexico
S. Carrillo Moreno, F. Vazquez Valencia

Benemerita Universidad Autonoma de Puebla, Puebla, Mexico
H.A. Salazar Ibarguen

Universidad Autónoma de San Luis Potosí, San Luis Potosí, Mexico
E. Casimiro Linares, A. Morelos Pineda, M.A. Reyes-Santos

University of Auckland, Auckland, New Zealand
D. Krofcheck

University of Canterbury, Christchurch, New Zealand
A.J. Bell, P.H. Butler, R. Doesburg, S. Reucroft, H. Silverwood

National Centre for Physics, Quaid-I-Azam University, Islamabad, Pakistan
M. Ahmad, M.I. Asghar, H.R. Hoorani, S. Khalid, W.A. Khan, T. Khurshid, S. Qazi, M.A. Shah, M. Shoaib

Institute of Experimental Physics, Faculty of Physics, University of Warsaw, Warsaw, Poland
G. Brona, M. Cwiok, W. Dominik, K. Doroba, A. Kalinowski, M. Konecki, J. Krolikowski

Soltan Institute for Nuclear Studies, Warsaw, Poland
H. Bialkowska, B. Boimska, T. Frueboes, R. Gokieli, M. Górski, M. Kazana, K. Nawrocki, K. Romanowska-Rybinska, M. Szleper, G. Wrochna, P. Zalewski

Laboratório de Instrumentação e Física Experimental de Partículas, Lisboa, Portugal
N. Almeida, P. Bargassa, A. David, P. Faccioli, P.G. Ferreira Parracho, M. Gallinaro, P. Musella, A. Nayak, J. Pela[1], J. Seixas, J. Varela, P. Vischia

Joint Institute for Nuclear Research, Dubna, Russia
I. Belotelov, P. Bunin, M. Gavrilenko, I. Golutvin, I. Gorbunov, A. Kamenev, V. Karjavin, G. Kozlov, A. Lanev, A. Malakhov, P. Moisenz, V. Palichik, V. Perelygin, S. Shmatov, V. Smirnov, A. Volodko, A. Zarubin

Petersburg Nuclear Physics Institute, Gatchina (St Petersburg), Russia
S. Evstyukhin, V. Golovtsov, Y. Ivanov, V. Kim, P. Levchenko, V. Murzin, V. Oreshkin, I. Smirnov, V. Sulimov, L. Uvarov, S. Vavilov, A. Vorobyev, An. Vorobyev

Institute for Nuclear Research, Moscow, Russia
Yu. Andreev, A. Dermenev, S. Gninenko, N. Golubev, M. Kirsanov, N. Krasnikov, V. Matveev, A. Pashenkov, D. Tlisov, A. Toropin

Institute for Theoretical and Experimental Physics, Moscow, Russia
V. Epshteyn, M. Erofeeva, V. Gavrilov, M. Kossov[1], N. Lychkovskaya, V. Popov, G. Safronov, S. Semenov, V. Stolin, E. Vlasov, A. Zhokin

Moscow State University, Moscow, Russia
A. Belyaev, E. Boos, V. Bunichev, M. Dubinin[4], L. Dudko, A. Ershov, A. Gribushin, V. Klyukhin, I. Lokhtin, A. Markina, S. Obraztsov, M. Perfilov, S. Petrushanko, L. Sarycheva†, V. Savrin, A. Snigirev

P.N. Lebedev Physical Institute, Moscow, Russia
V. Andreev, M. Azarkin, I. Dremin, M. Kirakosyan, A. Leonidov, G. Mesyats, S.V. Rusakov, A. Vinogradov

State Research Center of Russian Federation, Institute for High Energy Physics, Protvino, Russia
I. Azhgirey, I. Bayshev, S. Bitioukov, V. Grishin[1], V. Kachanov, D. Konstantinov, A. Korablev, V. Krychkine, V. Petrov, R. Ryutin, A. Sobol, L. Tourtchanovitch, S. Troshin, N. Tyurin, A. Uzunian, A. Volkov

University of Belgrade, Faculty of Physics and Vinca Institute of Nuclear Sciences, Belgrade, Serbia
P. Adzic[31], M. Djordjevic, M. Ekmedzic, D. Krpic[31], J. Milosevic

Centro de Investigaciones Energéticas Medioambientales y Tecnológicas (CIEMAT), Madrid, Spain
M. Aguilar-Benitez, J. Alcaraz Maestre, P. Arce, C. Battilana, E. Calvo, M. Cerrada, M. Chamizo Llatas, N. Colino, B. De La Cruz, A. Delgado Peris, C. Diez Pardos, D. Domínguez Vázquez, C. Fernandez Bedoya, J.P. Fernández Ramos, A. Ferrando, J. Flix, M.C. Fouz, P. Garcia-Abia, O. Gonzalez Lopez, S. Goy Lopez, J.M. Hernandez, M.I. Josa, G. Merino, J. Puerta Pelayo, I. Redondo, L. Romero, J. Santaolalla, M.S. Soares, C. Willmott

Universidad Autónoma de Madrid, Madrid, Spain
C. Albajar, G. Codispoti, J.F. de Trocóniz

Universidad de Oviedo, Oviedo, Spain
J. Cuevas, J. Fernandez Menendez, S. Folgueras, I. Gonzalez Caballero, L. Lloret Iglesias, J. Piedra Gomez[32], J.M. Vizan Garcia

Instituto de Física de Cantabria (IFCA), CSIC-Universidad de Cantabria, Santander, Spain
J.A. Brochero Cifuentes, I.J. Cabrillo, A. Calderon, S.H. Chuang, J. Duarte Campderros, M. Felcini[33], M. Fernandez, G. Gomez, J. Gonzalez Sanchez, C. Jorda, P. Lobelle Pardo, A. Lopez Virto, J. Marco, R. Marco, C. Martinez Rivero, F. Matorras, F.J. Munoz Sanchez, T. Rodrigo, A.Y. Rodríguez-Marrero, A. Ruiz-Jimeno, L. Scodellaro, M. Sobron Sanudo, I. Vila, R. Vilar Cortabitarte

CERN, European Organization for Nuclear Research, Geneva, Switzerland
D. Abbaneo, E. Auffray, G. Auzinger, P. Baillon, A.H. Ball, D. Barney, C. Bernet[5], G. Bianchi, P. Bloch, A. Bocci, A. Bonato, H. Breuker, K. Bunkowski, T. Camporesi, G. Cerminara, T. Christiansen, J.A. Coarasa Perez, D. D'Enterria, A. De Roeck, S. Di Guida, M. Dobson, N. Dupont-Sagorin, A. Elliott-Peisert, B. Frisch, W. Funk, G. Georgiou, M. Giffels, D. Gigi, K. Gill, D. Giordano, M. Giunta, F. Glege, R. Gomez-Reino Garrido, P. Govoni, S. Gowdy, R. Guida, M. Hansen, P. Harris, C. Hartl, J. Harvey, B. Hegner, A. Hinzmann, V. Innocente, P. Janot, K. Kaadze, E. Karavakis, K. Kousouris, P. Lecoq, P. Lenzi, C. Lourenço, T. Mäki, M. Malberti, L. Malgeri, M. Mannelli, L. Masetti, F. Meijers, S. Mersi, E. Meschi, R. Moser, M.U. Mozer, M. Mulders, E. Nesvold, M. Nguyen, T. Orimoto, L. Orsini, E. Palencia Cortezon, E. Perez, A. Petrilli, A. Pfeiffer, M. Pierini, M. Pimiä, D. Piparo, G. Polese, L. Quertenmont, A. Racz, W. Reece, J. Rodrigues Antunes, G. Rolandi[34], T. Rommerskirchen, C. Rovelli[35], M. Rovere, H. Sakulin, F. Santanastasio, C. Schäfer, C. Schwick, I. Segoni, S. Sekmen, A. Sharma, P. Siegrist, P. Silva, M. Simon, P. Sphicas[36], D. Spiga, M. Spiropulu[4], M. Stoye, A. Tsirou, G.I. Veres[17], J.R. Vlimant, H.K. Wöhri, S.D. Worm[37], W.D. Zeuner

Paul Scherrer Institut, Villigen, Switzerland
W. Bertl, K. Deiters, W. Erdmann, K. Gabathuler, R. Horisberger, Q. Ingram, H.C. Kaestli, S. König, D. Kotlinski, U. Langenegger, F. Meier, D. Renker, T. Rohe, J. Sibille[38]

Institute for Particle Physics, ETH Zurich, Zurich, Switzerland
L. Bäni, P. Bortignon, M.A. Buchmann, B. Casal, N. Chanon, Z. Chen, A. Deisher, G. Dissertori, M. Dittmar, M. Dünser, J. Eugster, K. Freudenreich, C. Grab, P. Lecomte, W. Lustermann, A.C. Marini, P. Martinez Ruiz del Arbol, N. Mohr, F. Moortgat, C. Nägeli[39], P. Nef, F. Nessi-Tedaldi, L. Pape, F. Pauss, M. Peruzzi, F.J. Ronga, M. Rossini, L. Sala, A.K. Sanchez, M.-C. Sawley, A. Starodumov[40], B. Stieger, M. Takahashi, L. Tauscher[†], A. Thea, K. Theofilatos, D. Treille, C. Urscheler, R. Wallny, H.A. Weber, L. Wehrli

Universität Zürich, Zurich, Switzerland
E. Aguilo, C. Amsler, V. Chiochia, S. De Visscher, C. Favaro, M. Ivova Rikova, B. Millan Mejias, P. Otiougova, P. Robmann, H. Snoek, S. Tupputi, M. Verzetti

National Central University, Chung-Li, Taiwan
Y.H. Chang, K.H. Chen, A. Go, C.M. Kuo, S.W. Li, W. Lin, Z.K. Liu, Y.J. Lu, D. Mekterovic, R. Volpe, S.S. Yu

National Taiwan University (NTU), Taipei, Taiwan
P. Bartalini, P. Chang, Y.H. Chang, Y.W. Chang, Y. Chao, K.F. Chen, C. Dietz, U. Grundler, W.-S. Hou, Y. Hsiung, K.Y. Kao, Y.J. Lei, R.-S. Lu, D. Majumder, E. Petrakou, X. Shi, J.G. Shiu, Y.M. Tzeng, M. Wang

Cukurova University, Adana, Turkey
A. Adiguzel, M.N. Bakirci[41], S. Cerci[42], C. Dozen, I. Dumanoglu, E. Eskut, S. Girgis, G. Gokbulut, I. Hos, E.E. Kangal, G. Karapinar, A. Kayis Topaksu, G. Onengut, K. Ozdemir, S. Ozturk[43], A. Polatoz, K. Sogut[44], D. Sunar Cerci[42], B. Tali[42], H. Topakli[41], L.N. Vergili, M. Vergili

Middle East Technical University, Physics Department, Ankara, Turkey
I.V. Akin, T. Aliev, B. Bilin, S. Bilmis, M. Deniz, H. Gamsizkan, A.M. Guler, K. Ocalan, A. Ozpineci, M. Serin, R. Sever, U.E. Surat, M. Yalvac, E. Yildirim, M. Zeyrek

Bogazici University, Istanbul, Turkey
M. Deliomeroglu, E. Gülmez, B. Isildak, M. Kaya[45], O. Kaya[45], S. Ozkorucuklu[46], N. Sonmez[47]

Istanbul Technical University, Istanbul, Turkey
K. Cankocak

National Scientific Center, Kharkov Institute of Physics and Technology, Kharkov, Ukraine
L. Levchuk

University of Bristol, Bristol, United Kingdom
F. Bostock, J.J. Brooke, E. Clement, D. Cussans, H. Flacher, R. Frazier, J. Goldstein, M. Grimes, G.P. Heath, H.F. Heath, L. Kreczko, S. Metson, D.M. Newbold[37], K. Nirunpong, A. Poll, S. Senkin, V.J. Smith, T. Williams

Rutherford Appleton Laboratory, Didcot, United Kingdom
L. Basso[48], K.W. Bell, A. Belyaev[48], C. Brew, R.M. Brown, D.J.A. Cockerill, J.A. Coughlan, K. Harder, S. Harper, J. Jackson, B.W. Kennedy, E. Olaiya, D. Petyt, B.C. Radburn-Smith, C.H. Shepherd-Themistocleous, I.R. Tomalin, W.J. Womersley

Imperial College, London, United Kingdom
R. Bainbridge, G. Ball, R. Beuselinck, O. Buchmuller, D. Colling, N. Cripps, M. Cutajar, P. Dauncey, G. Davies, M. Della Negra, W. Ferguson, J. Fulcher, D. Futyan, A. Gilbert, A. Guneratne Bryer, G. Hall, Z. Hatherell, J. Hays, G. Iles, M. Jarvis, G. Karapostoli, L. Lyons, A.-M. Magnan, J. Marrouche, B. Mathias, R. Nandi, J. Nash, A. Nikitenko[40], A. Papageorgiou, M. Pesaresi, K. Petridis, M. Pioppi[49], D.M. Raymond, S. Rogerson, N. Rompotis, A. Rose, M.J. Ryan, C. Seez, P. Sharp, A. Sparrow, A. Tapper, M. Vazquez Acosta, T. Virdee, S. Wakefield, N. Wardle, T. Whyntie

Brunel University, Uxbridge, United Kingdom
M. Barrett, M. Chadwick, J.E. Cole, P.R. Hobson, A. Khan, P. Kyberd, D. Leggat, D. Leslie, W. Martin, I.D. Reid, P. Symonds, L. Teodorescu, M. Turner

Baylor University, Waco, USA
K. Hatakeyama, H. Liu, T. Scarborough

The University of Alabama, Tuscaloosa, USA
C. Henderson, P. Rumerio

Boston University, Boston, USA
A. Avetisyan, T. Bose, C. Fantasia, A. Heister, J. St. John, P. Lawson, D. Lazic, J. Rohlf, D. Sperka, L. Sulak

Brown University, Providence, USA
J. Alimena, S. Bhattacharya, D. Cutts, A. Ferapontov, U. Heintz, S. Jabeen, G. Kukartsev, G. Landsberg, M. Luk, M. Narain, D. Nguyen, M. Segala, T. Sinthuprasith, T. Speer, K.V. Tsang

University of California, Davis, Davis, USA
R. Breedon, G. Breto, M. Calderon De La Barca Sanchez, S. Chauhan, M. Chertok, J. Conway, R. Conway, P.T. Cox, J. Dolen, R. Erbacher, M. Gardner, R. Houtz, W. Ko, A. Kopecky, R. Lander, O. Mall, T. Miceli, R. Nelson, D. Pellett, B. Rutherford, M. Searle, J. Smith, M. Squires, M. Tripathi, R. Vasquez Sierra

University of California, Los Angeles, Los Angeles, USA
V. Andreev, D. Cline, R. Cousins, J. Duris, S. Erhan, P. Everaerts, C. Farrell, J. Hauser, M. Ignatenko, C. Plager, G. Rakness, P. Schlein†, J. Tucker, V. Valuev, M. Weber

University of California, Riverside, Riverside, USA
J. Babb, R. Clare, M.E. Dinardo, J. Ellison, J.W. Gary, F. Giordano, G. Hanson, G.Y. Jeng[50], H. Liu, O.R. Long, A. Luthra, H. Nguyen, S. Paramesvaran, J. Sturdy, S. Sumowidagdo, R. Wilken, S. Wimpenny

University of California, San Diego, La Jolla, USA
W. Andrews, J.G. Branson, G.B. Cerati, S. Cittolin, D. Evans, F. Golf, A. Holzner, R. Kelley, M. Lebourgeois, J. Letts, I. Macneill, B. Mangano, J. Muelmenstaedt, S. Padhi, C. Palmer, G. Petrucciani, M. Pieri, R. Ranieri, M. Sani, V. Sharma, S. Simon, E. Sudano, M. Tadel, Y. Tu, A. Vartak, S. Wasserbaech[51], F. Würthwein, A. Yagil, J. Yoo

University of California, Santa Barbara, Santa Barbara, USA
D. Barge, R. Bellan, C. Campagnari, M. D'Alfonso, T. Danielson, K. Flowers, P. Geffert, J. Incandela, C. Justus, P. Kalavase, S.A. Koay, D. Kovalskyi[1], V. Krutelyov, S. Lowette, N. Mccoll, V. Pavlunin, F. Rebassoo, J. Ribnik, J. Richman, R. Rossin, D. Stuart, W. To, C. West

California Institute of Technology, Pasadena, USA
A. Apresyan, A. Bornheim, Y. Chen, E. Di Marco, J. Duarte, M. Gataullin, Y. Ma, A. Mott, H.B. Newman, C. Rogan, V. Timciuc, P. Traczyk, J. Veverka, R. Wilkinson, Y. Yang, R.Y. Zhu

Carnegie Mellon University, Pittsburgh, USA
B. Akgun, R. Carroll, T. Ferguson, Y. Iiyama, D.W. Jang, Y.F. Liu, M. Paulini, H. Vogel, I. Vorobiev

University of Colorado at Boulder, Boulder, USA
J.P. Cumalat, B.R. Drell, C.J. Edelmaier, W.T. Ford, A. Gaz, B. Heyburn, E. Luiggi Lopez, J.G. Smith, K. Stenson, K.A. Ulmer, S.R. Wagner

Cornell University, Ithaca, USA
L. Agostino, J. Alexander, A. Chatterjee, N. Eggert, L.K. Gibbons, B. Heltsley, W. Hopkins, A. Khukhunaishvili, B. Kreis, N. Mirman, G. Nicolas Kaufman, J.R. Patterson, A. Ryd, E. Salvati, W. Sun, W.D. Teo, J. Thom, J. Thompson, J. Vaughan, Y. Weng, L. Winstrom, P. Wittich

Fairfield University, Fairfield, USA
D. Winn

Fermi National Accelerator Laboratory, Batavia, USA
S. Abdullin, M. Albrow, J. Anderson, L.A.T. Bauerdick, A. Beretvas, J. Berryhill, P.C. Bhat, I. Bloch, K. Burkett, J.N. Butler, V. Chetluru, H.W.K. Cheung, F. Chlebana, V.D. Elvira, I. Fisk, J. Freeman, Y. Gao, D. Green, O. Gutsche, J. Hanlon, R.M. Harris, J. Hirschauer, B. Hooberman, S. Jindariani, M. Johnson, U. Joshi, B. Kilminster, B. Klima, S. Kunori, S. Kwan, D. Lincoln, R. Lipton, J. Lykken, K. Maeshima, J.M. Marraffino, S. Maruyama, D. Mason, P. McBride, K. Mishra, S. Mrenna, Y. Musienko[52], C. Newman-Holmes, V. O'Dell, O. Prokofyev, E. Sexton-Kennedy, S. Sharma, W.J. Spalding, L. Spiegel, P. Tan, L. Taylor, S. Tkaczyk, N.V. Tran, L. Uplegger, E.W. Vaandering, R. Vidal, J. Whitmore, W. Wu, F. Yang, F. Yumiceva, J.C. Yun

University of Florida, Gainesville, USA
D. Acosta, P. Avery, D. Bourilkov, M. Chen, S. Das, M. De Gruttola, G.P. Di Giovanni, D. Dobur, A. Drozdetskiy, R.D. Field, M. Fisher, Y. Fu, I.K. Furic, J. Gartner, J. Hugon, B. Kim, J. Konigsberg, A. Korytov, A. Kropivnitskaya, T. Kypreos, J.F. Low, K. Matchev, P. Milenovic[53], G. Mitselmakher, L. Muniz, R. Remington, A. Rinkevicius, P. Sellers, N. Skhirtladze, M. Snowball, J. Yelton, M. Zakaria

Florida International University, Miami, USA
V. Gaultney, L.M. Lebolo, S. Linn, P. Markowitz, G. Martinez, J.L. Rodriguez

Florida State University, Tallahassee, USA
T. Adams, A. Askew, J. Bochenek, J. Chen, B. Diamond, S.V. Gleyzer, J. Haas, S. Hagopian, V. Hagopian, M. Jenkins, K.F. Johnson, H. Prosper, V. Veeraraghavan, M. Weinberg

Florida Institute of Technology, Melbourne, USA
M.M. Baarmand, B. Dorney, M. Hohlmann, H. Kalakhety, I. Vodopiyanov

University of Illinois at Chicago (UIC), Chicago, USA
M.R. Adams, I.M. Anghel, L. Apanasevich, Y. Bai, V.E. Bazterra, R.R. Betts, J. Callner, R. Cavanaugh, C. Dragoiu, O. Evdokimov, E.J. Garcia-Solis, L. Gauthier, C.E. Gerber, D.J. Hofman, S. Khalatyan, F. Lacroix, M. Malek, C. O'Brien, C. Silkworth, D. Strom, N. Varelas

The University of Iowa, Iowa City, USA
U. Akgun, E.A. Albayrak, B. Bilki[54], K. Chung, W. Clarida, F. Duru, S. Griffiths, C.K. Lae, J.-P. Merlo, H. Mermerkaya[55], A. Mestvirishvili, A. Moeller, J. Nachtman, C.R. Newsom, E. Norbeck, J. Olson, Y. Onel, F. Ozok, S. Sen, E. Tiras, J. Wetzel, T. Yetkin, K. Yi

Johns Hopkins University, Baltimore, USA
B.A. Barnett, B. Blumenfeld, S. Bolognesi, D. Fehling, G. Giurgiu, A.V. Gritsan, Z.J. Guo, G. Hu, P. Maksimovic, S. Rappoccio, M. Swartz, A. Whitbeck

The University of Kansas, Lawrence, USA
P. Baringer, A. Bean, G. Benelli, O. Grachov, R.P. Kenny Iii, M. Murray, D. Noonan, V. Radicci, S. Sanders, R. Stringer, G. Tinti, J.S. Wood, V. Zhukova

Kansas State University, Manhattan, USA
A.F. Barfuss, T. Bolton, I. Chakaberia, A. Ivanov, S. Khalil, M. Makouski, Y. Maravin, S. Shrestha, I. Svintradze

Lawrence Livermore National Laboratory, Livermore, USA
J. Gronberg, D. Lange, D. Wright

University of Maryland, College Park, USA
A. Baden, M. Boutemeur, B. Calvert, S.C. Eno, J.A. Gomez, N.J. Hadley, R.G. Kellogg, M. Kirn, T. Kolberg, Y. Lu, M. Marionneau, A.C. Mignerey, A. Peterman, K. Rossato, A. Skuja, J. Temple, M.B. Tonjes, S.C. Tonwar, E. Twedt

Massachusetts Institute of Technology, Cambridge, USA
G. Bauer, J. Bendavid, W. Busza, E. Butz, I.A. Cali, M. Chan, V. Dutta, G. Gomez Ceballos, M. Goncharov, K.A. Hahn, Y. Kim, M. Klute, Y.-J. Lee, W. Li, P.D. Luckey, T. Ma, S. Nahn, C. Paus, D. Ralph, C. Roland, G. Roland, M. Rudolph, G.S.F. Stephans, F. Stöckli, K. Sumorok, K. Sung, D. Velicanu, E.A. Wenger, R. Wolf, B. Wyslouch, S. Xie, M. Yang, Y. Yilmaz, A.S. Yoon, M. Zanetti

University of Minnesota, Minneapolis, USA
S.I. Cooper, P. Cushman, B. Dahmes, A. De Benedetti, G. Franzoni, A. Gude, J. Haupt, S.C. Kao, K. Klapoetke, Y. Kubota, J. Mans, N. Pastika, V. Rekovic, R. Rusack, M. Sasseville, A. Singovsky, N. Tambe, J. Turkewitz

University of Mississippi, University, USA
L.M. Cremaldi, R. Kroeger, L. Perera, R. Rahmat, D.A. Sanders

University of Nebraska-Lincoln, Lincoln, USA
E. Avdeeva, K. Bloom, S. Bose, J. Butt, D.R. Claes, A. Dominguez, M. Eads, P. Jindal, J. Keller, I. Kravchenko, J. Lazo-Flores, H. Malbouisson, S. Malik, G.R. Snow

State University of New York at Buffalo, Buffalo, USA
U. Baur, A. Godshalk, I. Iashvili, S. Jain, A. Kharchilava, A. Kumar, S.P. Shipkowski, K. Smith

Northeastern University, Boston, USA
G. Alverson, E. Barberis, D. Baumgartel, M. Chasco, J. Haley, D. Trocino, D. Wood, J. Zhang

Northwestern University, Evanston, USA
A. Anastassov, A. Kubik, N. Mucia, N. Odell, R.A. Ofierzynski, B. Pollack, A. Pozdnyakov, M. Schmitt, S. Stoynev, M. Velasco, S. Won

University of Notre Dame, Notre Dame, USA
L. Antonelli, D. Berry, A. Brinkerhoff, M. Hildreth, C. Jessop, D.J. Karmgard, J. Kolb, K. Lannon, W. Luo, S. Lynch, N. Marinelli, D.M. Morse, T. Pearson, R. Ruchti, J. Slaunwhite, N. Valls, J. Warchol, M. Wayne, M. Wolf, J. Ziegler

The Ohio State University, Columbus, USA
B. Bylsma, L.S. Durkin, C. Hill, R. Hughes, P. Killewald, K. Kotov, T.Y. Ling, D. Puigh, M. Rodenburg, C. Vuosalo, G. Williams, B.L. Winer

Princeton University, Princeton, USA
N. Adam, E. Berry, P. Elmer, D. Gerbaudo, V. Halyo, P. Hebda, J. Hegeman, A. Hunt, E. Laird, D. Lopes Pegna, P. Lujan, D. Marlow, T. Medvedeva, M. Mooney, J. Olsen, P. Piroué, X. Quan, A. Raval, H. Saka, D. Stickland, C. Tully, J.S. Werner, A. Zuranski

University of Puerto Rico, Mayaguez, USA
J.G. Acosta, X.T. Huang, A. Lopez, H. Mendez, S. Oliveros, J.E. Ramirez Vargas, A. Zatserklyaniy

Purdue University, West Lafayette, USA
E. Alagoz, V.E. Barnes, D. Benedetti, G. Bolla, D. Bortoletto, M. De Mattia, A. Everett, Z. Hu, M. Jones, O. Koybasi, M. Kress, A.T. Laasanen, N. Leonardo, V. Maroussov, P. Merkel,

D.H. Miller, N. Neumeister, I. Shipsey, D. Silvers, A. Svyatkovskiy, M. Vidal Marono, H.D. Yoo, J. Zablocki, Y. Zheng

Purdue University Calumet, Hammond, USA
S. Guragain, N. Parashar

Rice University, Houston, USA
A. Adair, C. Boulahouache, V. Cuplov, K.M. Ecklund, F.J.M. Geurts, B.P. Padley, R. Redjimi, J. Roberts, J. Zabel

University of Rochester, Rochester, USA
B. Betchart, A. Bodek, Y.S. Chung, R. Covarelli, P. de Barbaro, R. Demina, Y. Eshaq, A. Garcia-Bellido, P. Goldenzweig, Y. Gotra, J. Han, A. Harel, S. Korjenevski, D.C. Miner, D. Vishnevskiy, M. Zielinski

The Rockefeller University, New York, USA
A. Bhatti, R. Ciesielski, L. Demortier, K. Goulianos, G. Lungu, S. Malik, C. Mesropian

Rutgers, the State University of New Jersey, Piscataway, USA
S. Arora, O. Atramentov, A. Barker, J.P. Chou, C. Contreras-Campana, E. Contreras-Campana, D. Duggan, D. Ferencek, Y. Gershtein, R. Gray, E. Halkiadakis, D. Hidas, D. Hits, A. Lath, S. Panwalkar, M. Park, R. Patel, A. Richards, J. Robles, K. Rose, S. Salur, S. Schnetzer, C. Seitz, S. Somalwar, R. Stone, S. Thomas

University of Tennessee, Knoxville, USA
G. Cerizza, M. Hollingsworth, S. Spanier, Z.C. Yang, A. York

Texas A&M University, College Station, USA
R. Eusebi, W. Flanagan, J. Gilmore, T. Kamon[56], V. Khotilovich, R. Montalvo, I. Osipenkov, Y. Pakhotin, A. Perloff, J. Roe, A. Safonov, T. Sakuma, S. Sengupta, I. Suarez, A. Tatarinov, D. Toback

Texas Tech University, Lubbock, USA
N. Akchurin, J. Damgov, P.R. Dudero, C. Jeong, K. Kovitanggoon, S.W. Lee, T. Libeiro, Y. Roh, I. Volobouev

Vanderbilt University, Nashville, USA
E. Appelt, D. Engh, C. Florez, S. Greene, A. Gurrola, W. Johns, P. Kurt, C. Maguire, A. Melo, P. Sheldon, B. Snook, S. Tuo, J. Velkovska

University of Virginia, Charlottesville, USA
M.W. Arenton, M. Balazs, S. Boutle, B. Cox, B. Francis, J. Goodell, R. Hirosky, A. Ledovskoy, C. Lin, C. Neu, J. Wood, R. Yohay

Wayne State University, Detroit, USA
S. Gollapinni, R. Harr, P.E. Karchin, C. Kottachchi Kankanamge Don, P. Lamichhane, A. Sakharov

University of Wisconsin, Madison, USA
M. Anderson, M. Bachtis, D. Belknap, L. Borrello, D. Carlsmith, M. Cepeda, S. Dasu, L. Gray, K.S. Grogg, M. Grothe, R. Hall-Wilton, M. Herndon, A. Hervé, P. Klabbers, J. Klukas, A. Lanaro, C. Lazaridis, J. Leonard, R. Loveless, A. Mohapatra, I. Ojalvo, G.A. Pierro, I. Ross, A. Savin, W.H. Smith, J. Swanson

†: Deceased
1: Also at CERN, European Organization for Nuclear Research, Geneva, Switzerland

2: Also at National Institute of Chemical Physics and Biophysics, Tallinn, Estonia
3: Also at Universidade Federal do ABC, Santo Andre, Brazil
4: Also at California Institute of Technology, Pasadena, USA
5: Also at Laboratoire Leprince-Ringuet, Ecole Polytechnique, IN2P3-CNRS, Palaiseau, France
6: Also at Suez Canal University, Suez, Egypt
7: Also at Zewail City of Science and Technology, Zewail, Egypt
8: Also at Cairo University, Cairo, Egypt
9: Also at British University, Cairo, Egypt
10: Also at Fayoum University, El-Fayoum, Egypt
11: Now at Ain Shams University, Cairo, Egypt
12: Also at Soltan Institute for Nuclear Studies, Warsaw, Poland
13: Also at Université de Haute-Alsace, Mulhouse, France
14: Also at Moscow State University, Moscow, Russia
15: Also at Brandenburg University of Technology, Cottbus, Germany
16: Also at Institute of Nuclear Research ATOMKI, Debrecen, Hungary
17: Also at Eötvös Loránd University, Budapest, Hungary
18: Also at Tata Institute of Fundamental Research - HECR, Mumbai, India
19: Now at King Abdulaziz University, Jeddah, Saudi Arabia
20: Also at University of Visva-Bharati, Santiniketan, India
21: Also at Sharif University of Technology, Tehran, Iran
22: Also at Isfahan University of Technology, Isfahan, Iran
23: Also at Shiraz University, Shiraz, Iran
24: Also at Plasma Physics Research Center, Science and Research Branch, Islamic Azad University, Teheran, Iran
25: Also at Facoltà Ingegneria Università di Roma, Roma, Italy
26: Also at Università della Basilicata, Potenza, Italy
27: Also at Università degli Studi Guglielmo Marconi, Roma, Italy
28: Also at Laboratori Nazionali di Legnaro dell' INFN, Legnaro, Italy
29: Also at Università degli studi di Siena, Siena, Italy
30: Also at University of Bucharest, Bucuresti-Magurele, Romania
31: Also at Faculty of Physics of University of Belgrade, Belgrade, Serbia
32: Also at University of Florida, Gainesville, USA
33: Also at University of California, Los Angeles, Los Angeles, USA
34: Also at Scuola Normale e Sezione dell' INFN, Pisa, Italy
35: Also at INFN Sezione di Roma; Università di Roma "La Sapienza", Roma, Italy
36: Also at University of Athens, Athens, Greece
37: Also at Rutherford Appleton Laboratory, Didcot, United Kingdom
38: Also at The University of Kansas, Lawrence, USA
39: Also at Paul Scherrer Institut, Villigen, Switzerland
40: Also at Institute for Theoretical and Experimental Physics, Moscow, Russia
41: Also at Gaziosmanpasa University, Tokat, Turkey
42: Also at Adiyaman University, Adiyaman, Turkey
43: Also at The University of Iowa, Iowa City, USA
44: Also at Mersin University, Mersin, Turkey
45: Also at Kafkas University, Kars, Turkey
46: Also at Suleyman Demirel University, Isparta, Turkey
47: Also at Ege University, Izmir, Turkey
48: Also at School of Physics and Astronomy, University of Southampton, Southampton, United Kingdom

49: Also at INFN Sezione di Perugia; Università di Perugia, Perugia, Italy
50: Also at University of Sydney, Sydney, Australia
51: Also at Utah Valley University, Orem, USA
52: Also at Institute for Nuclear Research, Moscow, Russia
53: Also at University of Belgrade, Faculty of Physics and Vinca Institute of Nuclear Sciences, Belgrade, Serbia
54: Also at Argonne National Laboratory, Argonne, USA
55: Also at Erzincan University, Erzincan, Turkey
56: Also at Kyungpook National University, Daegu, Korea